Atomic Energy Control Board
P.O. Box 1046
Ottawa, Canada
K1P 5S9

Commission de contrôle de l'énergie atomique
C.P. 1046
Ottawa, Canada
K1P 5S9

INFO-0335

# THE EFFECT OF HIGH-FREQUENCY GROUND MOTION ON THE MAPLE-X10 REACTOR

by

S. Bhan and S. Dunbar
Acres International Limited

A research report prepared for the
Atomic Energy Control Board
Ottawa, Canada

Project No. 2.183.1

June 1989

Canada

Research report

90-04394/

# The Effect of High-Frequency Ground Motion on the Maple-X10 Reactor

A report prepared by Acres International Limited under contract to the Atomic Energy Control Board.

## Abstract

The effect of high-frequency ground motion on structures and equipment in nuclear reactors is examined by subjecting simple linear models to selected recorded ground motions which exhibit low and high frequencies. Computed damage measures indicate that high-frequency short-duration ground motion, such as that observed in eastern North America have a minimal effect on structures with low natural frequencies. Response spectra of high-frequency ground motion indicate that higher forces are induced in structures with high natural frequencies as compared to those induced by low-frequency ground motion. However, reported observations of earthquake damage in eastern North America suggest that high-frequency ground motion causes little or no damage to structures. This may be due to the energy absorption capability of structures.

It is concluded that the response spectrum representative of ground motion observed in eastern North America may give an over-conservative measure of the response of structures with high natural frequencies, since it does not account for the typically observed short duration of high-frequency ground motion and for the energy absorption capability of structures. Detailed nonlinear analysis of specific structures with high natural frequencies should be performed to better predict the actual response. Recommendations for a nonlinear analysis of typical structures with high natural frequencies are made.

## Résumé

Dans le présent rapport, les chercheurs ont étudié l'action des mouvements de sol à hautes fréquences sur les structures et le matériel des réacteurs nucléaires en faisant subir à des modèles linéaires simples certains mouvements de sol enregistrés à basses et hautes fréquences. Les mesures informatisées des dommages indiquent que les mouvements de sol à hautes fréquences et de courte durée, tel qu'on a noté dans l'est de l'Amérique du Nord, exercent une action minime sur des structures à basses fréquences naturelles. Les spectres de réponse de mouvements de sol à hautes fréquences indiquent que des forces plus élevées sont provoquées dans les structures à hautes fréquences naturelles par comparaison aux forces provoquées par les mouvements de sol à basses fréquences. Or, les observations qu'on a rapportées en ce qui concerne les dommages causés par des tremblements de terre dans l'est de l'Amérique du Nord laissent supposer que les mouvements de sol à hautes fréquences causent peu ou pas de dommage aux structures. Cette situation peut être expliquée par la capacité des structures d'absorber de l'energie.

Les chercheurs sont arrivés à la conclusion que le spectre de réponse représentatif de mouvement de sol dans l'est de l'Amérique du Nord peut donner une estimation trop prudente de la réponse des structures à hautes fréquences naturelles parce qu'il ne tient pas

compte de la courte durée des mouvements typiques de sol à hautes fréquences et de la capacité des structures d'absorber de l'énergie. Pour déterminer la réponse réelle, il serait nécessaire de réaliser une analyse non linéaire détaillée de structures spécifiques à hautes fréquences naturelles. Le rapport apporte des recommandations pour l'analyse des structures spécifiques à hautes fréquences naturelles.

---

## Disclaimer

The Atomic Energy Control Board is not responsible for the accuracy of the statements made or opinions expressed in this publication and neither the Board nor the author assumes liability with respect to any damage or loss incurred as a result of the use made of the information contained in this publication.

# Table of Contents

A. Introduction . . . . . 1
1. Background . . . . . 1
2. Outline and Scope of Report . . . . . 6
3. Selected Accelerograms . . . . . 6
3.1. Kern County, California, 1952 . . . . . 7
3.2. Parkfield, California, 1966 . . . . . 7
3.3. Miramichi, New Brunswick, 1982 . . . . . 12
3.4. Nahanni, NWT, 1985 . . . . . 12
3.5. Leroy, Ohio, 1986 . . . . . 12
3.6. Saguenay, Quebec, 1988 . . . . . 12

B. Review of Damage Criteria . . . . . 13
1. Damage Measures for Observed Ground Motion . . . . . 13
1.1. Mercalli Intensity Scale . . . . . 13
1.2. Peak Ground Motion . . . . . 14
1.3. Effective Ground Motion . . . . . 14
1.4. Duration and RMS Acceleration . . . . . 15
1.5. Arias Intensity . . . . . 18
1.6. Cumulative Absolute Velocity . . . . . 18
2. Damage Measures for Structural Models . . . . . 21
2.1. Maximum Allowable Stress or Deformation . . . . . 21
2.2. Displacement Ductility . . . . . 22
2.3. Cumulative Damage and and Fatigue Failure Mechanisms . . . . . 23
2.4. Energy Absorption and Dissipation . . . . . 25
2.5. Empirical Damage Measures . . . . . 26
3. Discussion . . . . . 27

C. Analyses of Model Structures . . . . . 30
1. SDOF Models . . . . . 30
1.1. Response Spectra . . . . . 30
1.2. Energy Spectra . . . . . 31
1.3. Blast Damage Threshold Criterion . . . . . 33
1.4. Discussion . . . . . 36
2. MDOF Model . . . . . 38
3. Implications for the Maple-X10 Reactor. . . . . 43

D. Conclusions and Recommendations . . . . . 46
1. Conclusions . . . . . 46
2. Recommendations . . . . . 47

REFERENCES

APPENDIX A - RESPONSE SPECTRA

# The Effect of High-Frequency Ground Motion on the Maple X-10 Reactor

## A. Introduction

### 1. Background

Atomic Energy of Canada Ltd (AECL) is planning to build the Maple-X10 Research Reactor at Chalk River, Ontario. The seismic design of the reactor is based on CSA Standard CAN3-N289.3-M81 [Ref 1]. The design response spectrum in the CSA standard is based on accelerogram records from western North America (WNA). However, recent observations suggest that accelerograms in eastern North America (ENA) exhibit significantly higher frequencies (>10 Hz) than those in WNA. If this is the case, the design spectrum in the CSA standard would be deficient at higher frequencies.

The Atomic Energy Control Board (AECB), the licensing authority for nuclear reactors in Canada, has tasked Acres International Limited (AIL) to examine the effect of high-frequency ground motion on the reactor which exhibits natural frequencies exceeding 15 Hz.

Acccording to Ref 1, seismic design begins with establishing a Design Basis Earthquake (DBE). Ground motions associated with the DBE are then emplc,ed for the seismic qualification of safety-related structures and equipment (i.e., such structures and equipment must survive the occurrence of the DBE).

The ground motion is typically defined in terms of a response spectrum. As few or no data are available to determine response spectra at a particular site, it is common to use standard response spectra which are the response of a single degree of freedom oscillator normalized by peak values of ground motion. These standard spectra are developed by a statistical analysis of response spectra of existing accelerograms recorded from past earthquakes. Thus, given values of peak ground displacement (PGD), peak ground velocity (PGV) and peak ground acceleration (PGA), the standard spectra are scaled by these peak values to produce the design spectrum. An example of this procedure is shown in Figure 1. Further details may be found in Ref 2. The theory of the response spectrum is presented in Appendix A.

As stated above the standard spectra have been developed by a statistical analysis of response spectra computed from accelerograms of past earthquakes, the majority of which are from WNA [Refs 2, 3, 4 and 5]. However, as mentioned above, there is growing evidence that the amplitudes of these spectra in the high frequency range (>10 Hz) are not representative of earthquakes in ENA. Figure 2-1 shows the accelerogram and response spectrum of the 1949 Hollister, California M5.3 earthquake, which is representative of ground motion recorded in WNA. Figure 2-2 shows the accelerogram and response spectra of the 1986 Leroy, Ohio M4.8 earthquake, which is representative of observed high-frequency ground motion recorded in ENA.

Although of similar magnitude and recorded at similar epicentral distances, the frequency content of the two earthquakes is apparently quite different. The qualifier 'apparently' is necessary because the bandwidth of the accelerometers which recorded these earthquakes is probably quite different; the 1949 Hollister accelerometer was probably not capable of accurately recording frequencies much greater than 15 Hz, even if they existed.

Nevertheless, the differences between the two spectra are significant and not easily explained by differences in recording technology alone. In general, earth materials act as a low pass filter such that high frequencies tend to be attenuated with distance. Indeed, the duration of high-frequency ground motion shown in the accelerogram of Figure 2-2 is relatively short. This is typical of most accelerograms observed in ENA to date. The persistence with distance high-frequency ground motion in ENA is likely due to the homogeneous nature and high strength of crustal materials in ENA as compared to WNA [Refs 7, 8].

The Leroy, Ohio earthquake exceeded the operating limits of the Perry Nuclear Power Plant resulting in a delay in plant start-up, until it could be established that no damage had occurred. In fact no damage was observed or indicated and the plant finally began full operation about 2 months after the earthquake. Similar incidents have occurred at other reactors in the eastern US. This has caused the US Nuclear Regulatory Commission to reconsider its definition of exceedance of the Operating Basis Earthquake used to determine when to shut down a plant for inspection [Ref 6].

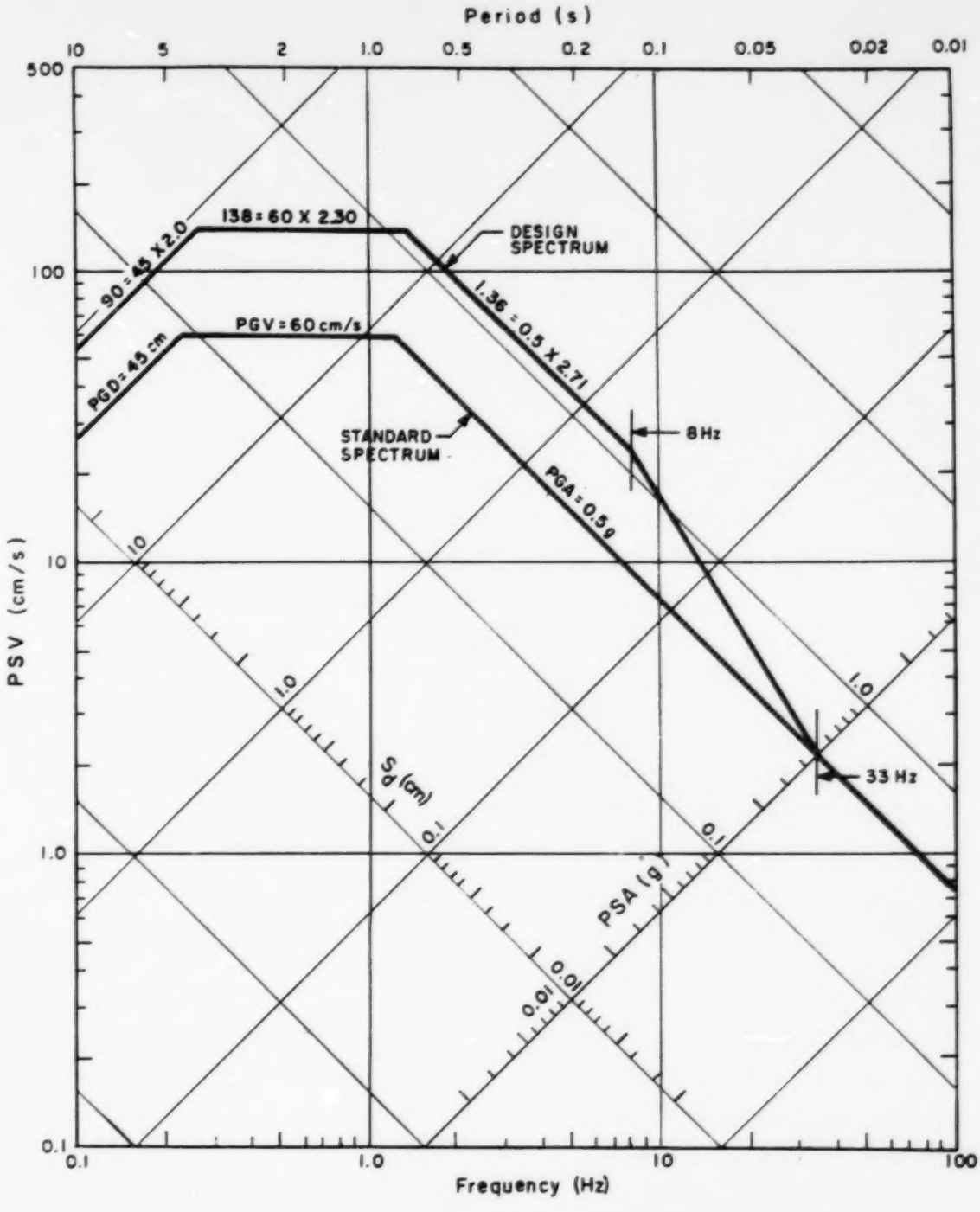


STANDARD SPECTRUM FROM REF 2

Fig. 1

Atomic Energy Control Board
The Effect of High Frequency Ground Motion on the Maple-X10 Reactor
Design Response Spectrum (5% Damping)

ACRES

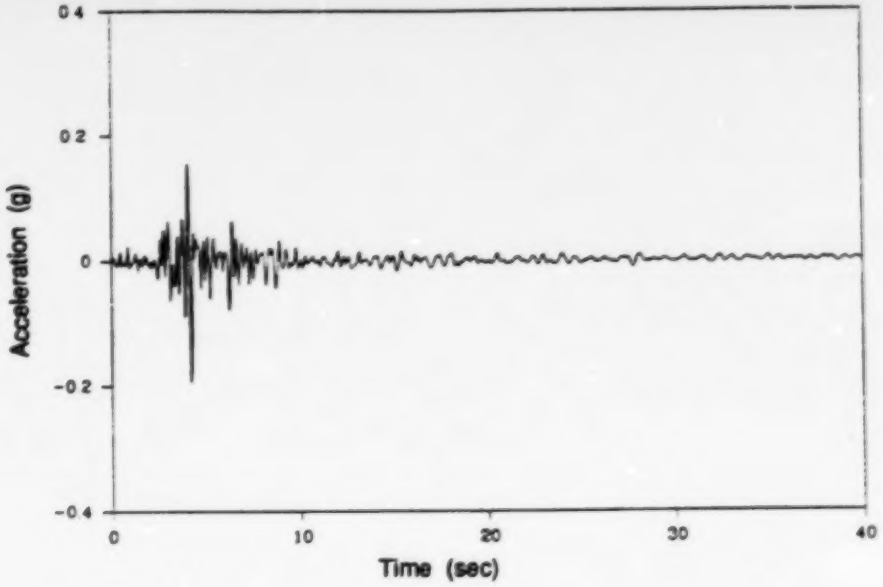


Accelerogram

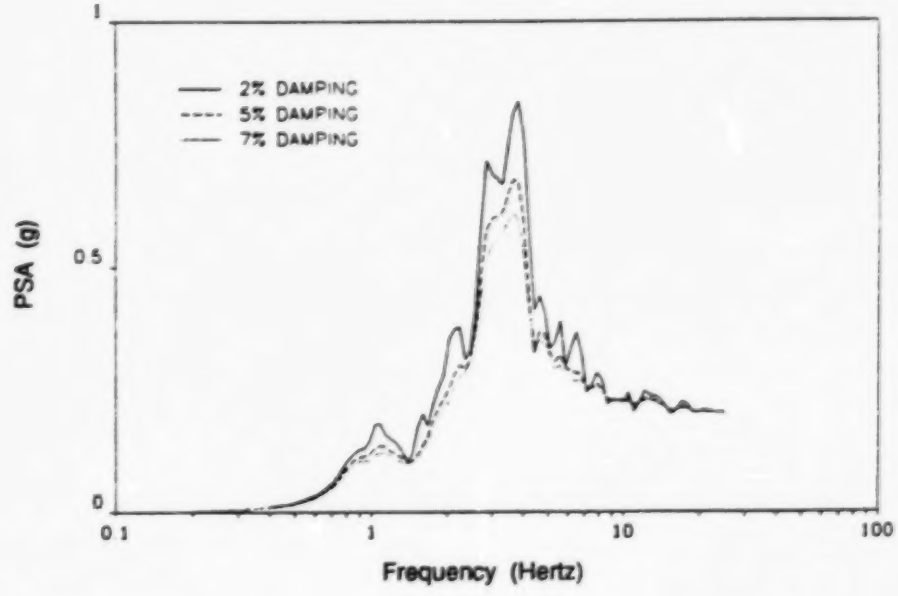


Response Spectra

Fig. 2-1

Atomic Energy Control Board
The Effect of High Frequency Ground Motion on the Maple-X10 Reactor
1949 Hollister, California Accelerogram and Response Spectra

ACRES

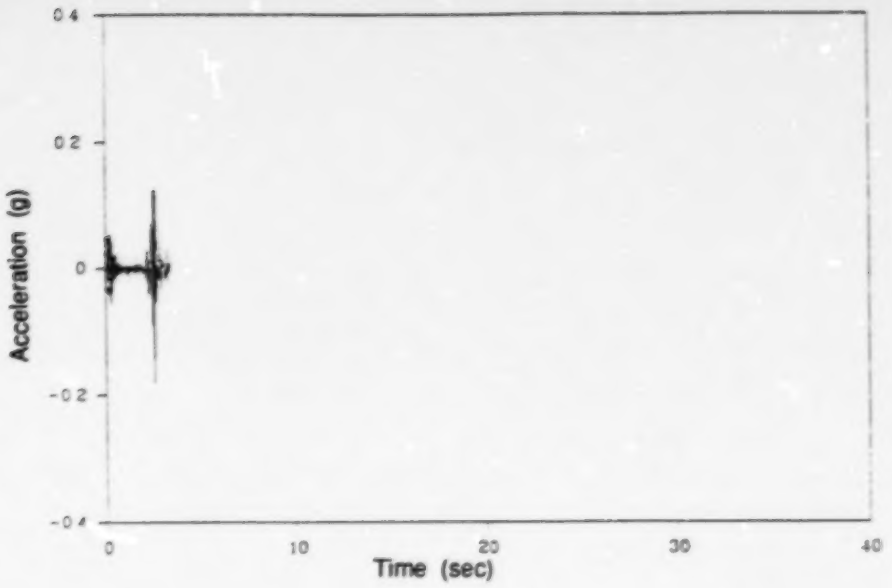


Accelerogram

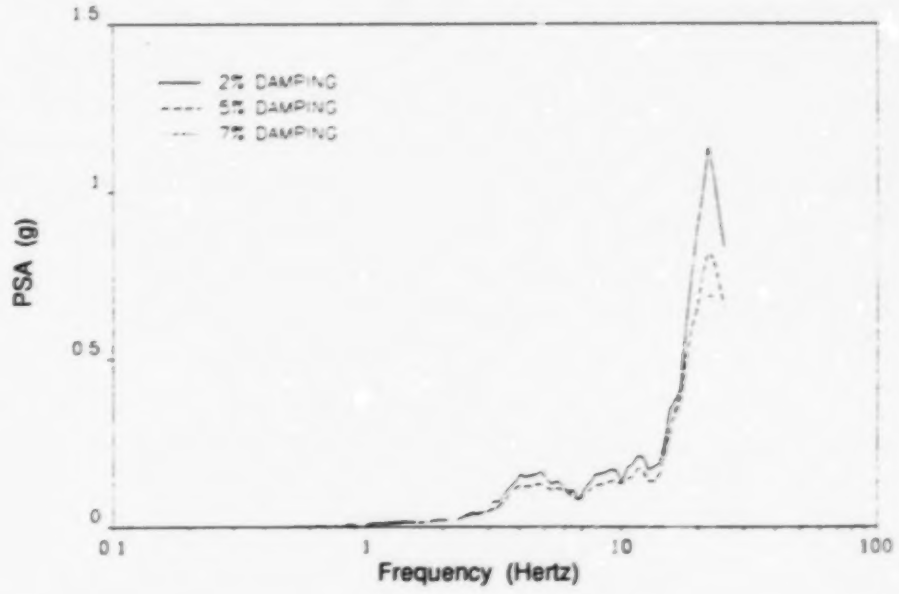


Response Spectra

Fig. 2-2

Atomic Energy Control Board
The Effect of High Frequency Ground Motion on the Maple-X10 Reactor
1986 Leroy, Ohio Accelerogram and Response Spectra

Although it is apparent that the effect of high-frequency ground motion on structures with low-natural frequencies (<10 Hz) is minimal, the same may not be true for structures and equipment in nuclear plants whose resonant frequencies are greater than 10 Hz. There is evidence [Refs 2, 6] that high-frequency ground motion does not cause damage and, therefore, response of modes greater than 10 Hz should be ignored in design. However, this needs to be verified. It is likely that the effect of high-frequency ground motion depends on the structure and materials in question.

## 2. Outline and Scope of Report

The first step in this analysis is to select representative accelerograms from both ENA and WNA. This is discussed in the next section.

To compare the effect of the two types of earthquakes of the design of a structure, it is necessary to have some measure of the damage potential of the computed response of the structure. A literature review of various damage measures is discussed in Chapter B.

In Chapter C the analyses of linear single degree of freedom (SDOF) systems and a linear multi-degree of freedom (MDOF) model are presented. Indicators of damage are computed for each computed motion. The implications of the results for the Maple-X10 reactor are discussed.

Finally, Chapter D gives conclusions resulting from this study and recommends a program of further research into the effects of high-frequency ground motion on specific structures.

## 3. Selected Accelerograms

Accelerograms recorded from six different earthquakes were selected. Table 1-1 lists the earthquakes and their magnitudes and epicentral distances. The horizontal components with the largest peak ground acceleration were used in the analyses. The time histories for these

components are presented in Figure 3. Response spectra at 2% and 5% damping for each of the accelerograms are presented in Figures 4-1 and 4-2 respectively.

Table 1-2 lists some index parameters of each earthquake. All of these, except the Nyquist frequency, will be described in Chapter B, 1. The Nyquist frequency, $f_N$, is the maximum frequency which the data is capable of representing. If t is the time sampling interval, then $f_N$ = 1/2 t (i.e., minimum two samples per wave length). However, for more recent earthquakes, recording and data processing techniques have increased the Nyquist frequency.

For the Kern County and Parkfield accelerograms, the time sampling interval t = 0.02 seconds. Given little information regarding the recording and processing of these records, this gives $f_N$ = 25 Hz for both records. For the other records, t = 0.005 seconds giving $f_N$ = 100 Hz. However, a high-cut filter is applied to the data so that frequencies between 50 and 100 Hz are attenuated. For this reason, the Nyquist of the post-1966 records is estimated to be 50 Hz. In any event, there is more high frequency (>25 Hz) content in these later accelerograms than in the older Kern County and Parkfield accelerograms.

Further details concerning these accelerograms are discussed in the following sections.

## 3.1. Kern County, California, 1952

The main reason for selection of this record is that it is considered to be a typical WNA event. Its magnitude (7.2) is rather large and probably not representative of the size of ENA events. Nevertheless it is useful for comparative purposes. This accelerogram was recorded on a soil site.

## 3.2. Parkfield, California, 1966

This record is also a typical WNA event. However its magnitude (6.5) is lower than that of Kern County. In addition, the epicentral distance from the recording station is much less than that of Kern County and thus the high-frequency content is probably greater than that of Kern County. This accelerogram was recorded on a soil site.

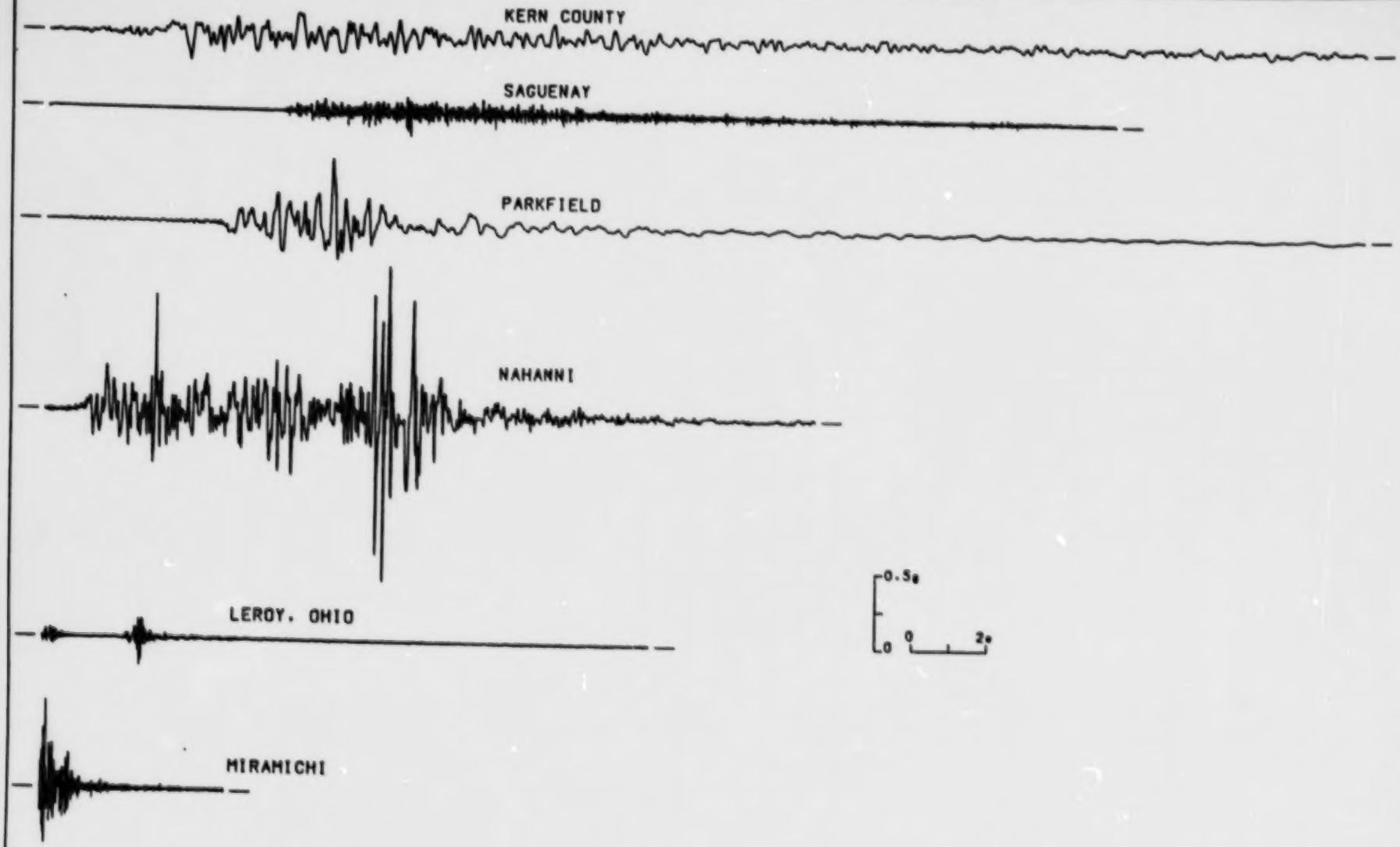


Fig. 3

Atomic Energy Control Board
The Effect of High Frequency Ground Motion on the Maple-X10 Reactor
Selected Accelerograms

**TABLE 1-1**

**SELECTED ACCELEROGRAMS**

| Event | Date | Station | Component | Δ (km) | $M$ |
|---|---|---|---|---|---|
| Kern County | 21/7/1952 | Taft Lincoln Tunnel | S69E | 40 | 7.2 |
| Saguenay | 25/11/1988 | St. Andre | N-S | 64 | 5.9 |
| Parkfield | 27/6/1966 | Cholame Shandon #5 | N85E | 5 | 6.1 |
| Nahanni | 23/12/1985 | Site 1 | N10E | 7 | 6.8 |
| Leroy, Ohio | 31/1/1986 | Perry Plant | N-S | 17 | 4.8 |
| Miramichi | 31/3/1982 | Loggie Lodge | S81E | 6 | 4.0 |

**TABLE 1-2**

**INDEX PARAMETERS OF SELECTED ACCELEROGRAMS**

| Event | PGA(g) | Duration (s)† | CAV (g-sec) | RMSA (g) | $f_N$ (Hz)‡ |
|---|---|---|---|---|---|
| Kern County | 0.18 | 28.86 | 0.92 | 0.03 | 25 |
| Saguenay | 0.16 | 12.58 | 0.31 | 0.03 | 50 |
| Parkfield | 0.42 | 6.74 | 0.67 | 0.09 | 25 |
| Nahanni | 1.10 | 7.92 | 1.32 | 0.19 | 50 |
| Leroy, Ohio | 0.18 | 5.62 | 0.09 | 0.02 | 50 |
| Miramichi | 0.58 | 0.82 | 0.11 | 0.13 | 50 |

†As defined in Ref 14

‡$f_N$ is the estimated Nyquist frequency of the available data.

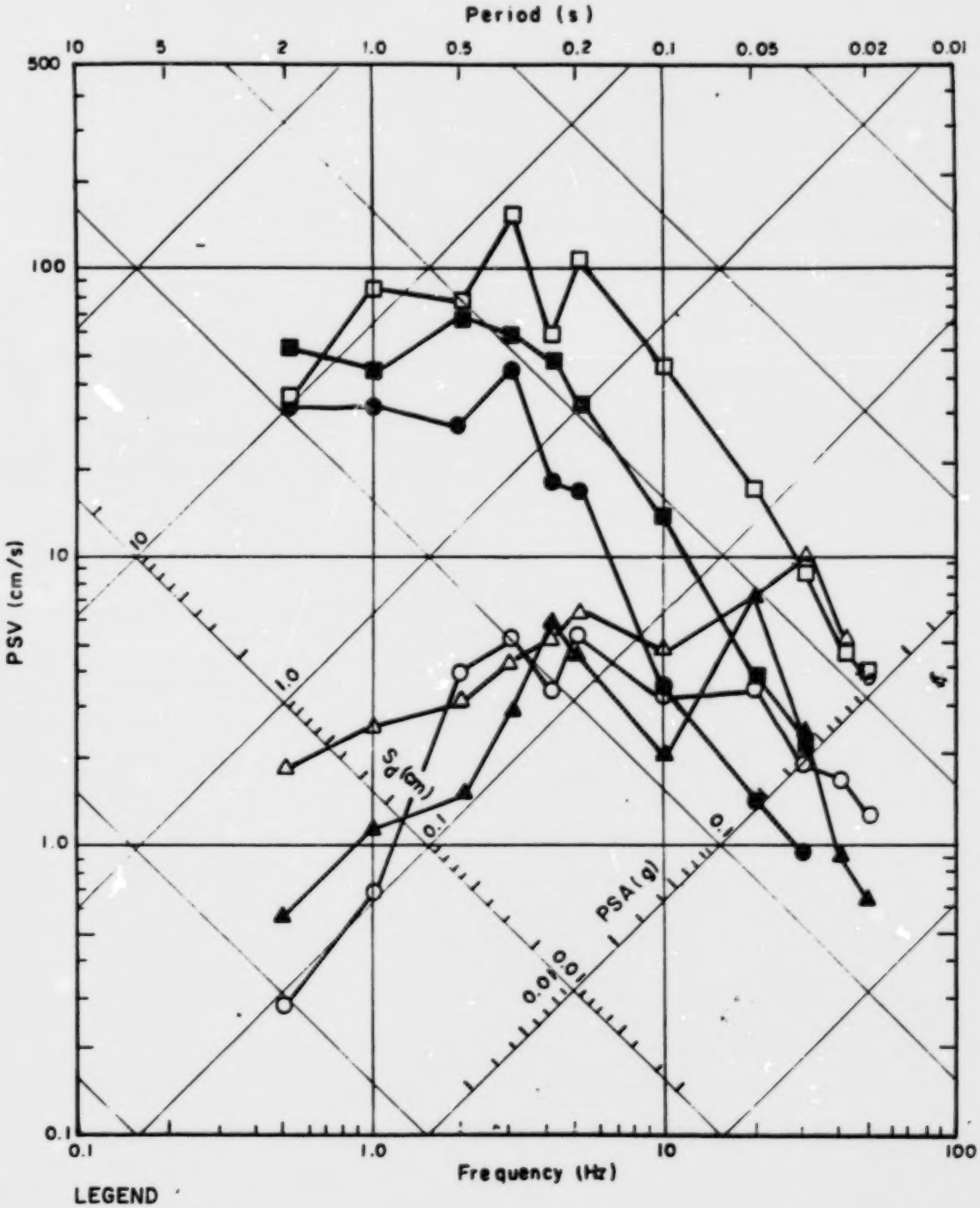


Fig. 4-1

Atomic Energy Control Board

The Effect of High Frequency Ground Motion on the Maple-X10 Reactor

Response Spectra of Selected Accelerograms (2% Damping)

ACRES

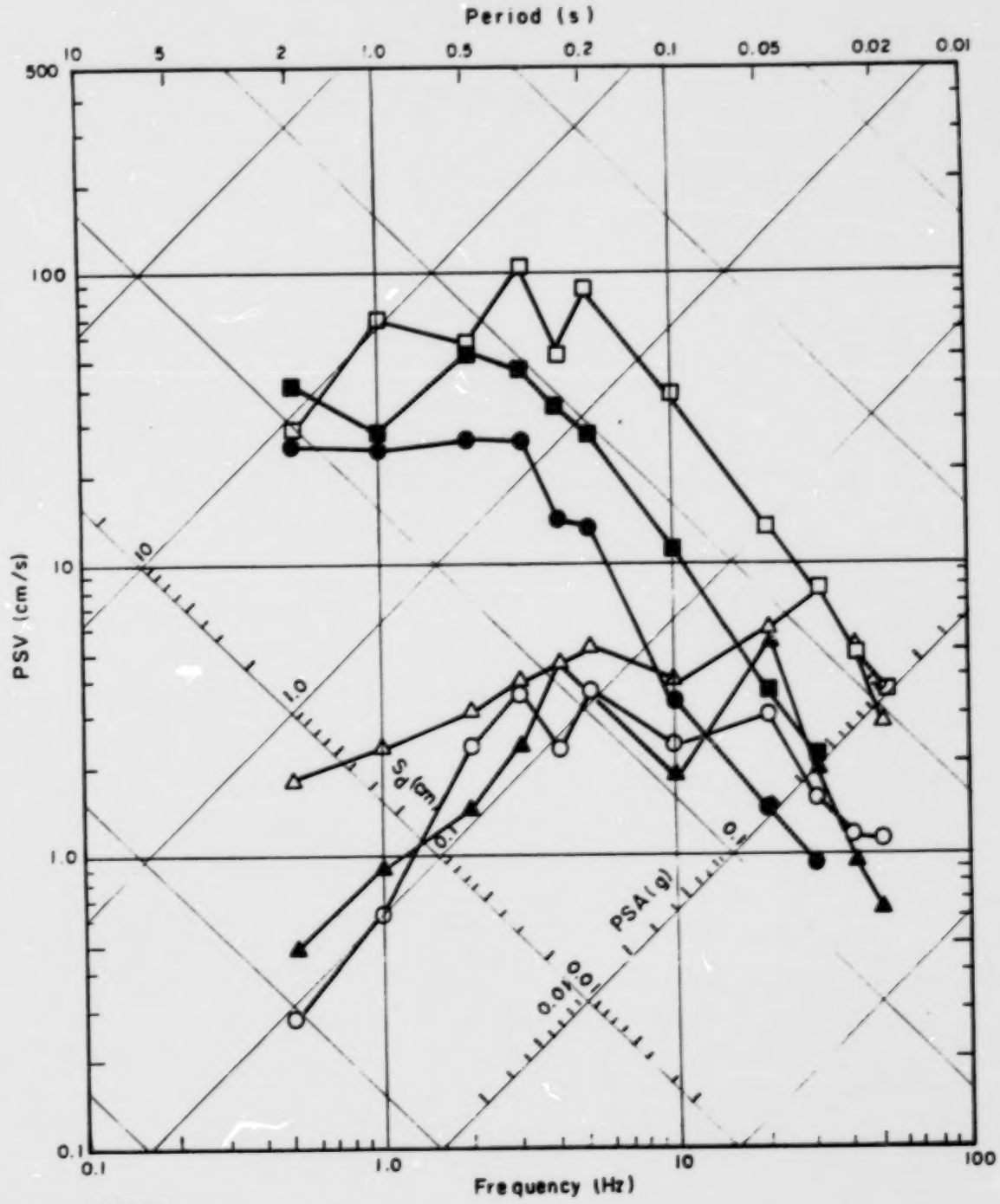


LEGEND

- ● KERN COUNTY
- ○ SAGUENAY
- ■ PARKFIELD
- □ NAHANNI
- ▲ LEROY, OHIO
- △ MIRAMICHI

Fig. 4-2

Atomic Energy Control Board

The Effect of High Frequency Ground Motion on the Maple-X10 Reactor

Response Spectra of Selected Accelerograms (5% Damping)

AECB

### 3.3. Miramichi, New Brunswick, 1982

The Miramichi sequence of earthquakes provided some excellent records in the very near field. Most of these records possess energy at quite high frequencies (approximately 40 Hz). Peak accelerations of these records are high but durations of significant ground motion are low. This record is considered representative of ground motion in ENA, at least in the near field. This accelerogram was recorded on a rock site.

### 3.4. Nahanni, NWT, 1985

This event produced very large peak accelerations at short epicentral distances. However, the duration of significant ground motion is longer than that of Miramichi, mainly because of the larger magnitude of this earthquake. There is some debate as to whether this is a typical ENA style earthquake. However, it does have a significant high-frequency content. This accelerogram was recorded on a rock site.

### 3.5. Leroy, Ohio, 1986

This earthquake is similar to Miramichi in that it is of similar magnitude and produced much high-frequency ground motion. It is considered to be a typical ENA event. This accelerogram was recorded on the basemat of the Perry Nuclear Power Plant in Ohio.

### 3.6. Saguenay, Quebec, 1988

This is the largest earthquake to have occurred in ENA in over 50 years. The duration of significant ground motion is long but the amplitudes are low. This accelerogram was recorded on a rock site.

For purposes of ENA-WNA comparisons, the pairs Nahanni-Parkfield and Kern County-Saguenay are appropriate. The Nahanni and Parkfield earthquakes have similar magnitudes and epicentral distances. Epicentral distances of the Kern County and Saguenay earthquakes are similar, although their magnitudes are different.

# B. Review of Damage Criteria

In this report, a distinction is made between measures of damage potential of ground motion to structures and measures of damage to a model of a structure. A further distinction is made between the above two measures and measures of damage for an existing structure subjected to an earthquake as the latter could involve considerations such as, for example, operability or economics of repair.

## 1. Damage Measures for Observed Ground Motion

Many attempts have been made to assess the damage potential of earthquakes based on observed ground motions. Such damage measures would be of obvious interest to operators of critical facilities where accelerometers are installed. However, the problem with defining a measure of damage based only on ground motion is that damage level is dependent on the nature of the structure or equipment and its design. In order to provide an appreciation of the difficulty of defining the damage potential of ground motion, several damage measures are discussed below in some detail.

### 1.1. Mercalli Intensity Scale

The first measure of earthquake damage was the Mercalli Intensity scale. This scale was first developed during the 30s and has since been modified to become the Modified Mercalli Intensity (MMI) scale [Refs 9, 10]. The scale is entirely empirical and consists of assigning numerical values (Roman numerals I through IX) to descriptions of damage to buildings. The main disadvantage of the scale is that the descriptions of damage used to define a particular intensity value are open to interpretation. However, the scale is still used and, if properly applied, can give a good description of the distribution of intensity around an earthquake.

## 1.2. Peak Ground Motion

Peak values of ground motion were the first quantitative measures of damage potential. If y(t) is the measured ground motion (acceleration, velocity or displacement), then the definition of the peak value of y, PY is

$$PY = \max_t |y(t)| \tag{B.1}$$

Note that a response spectral ordinate is a peak quantity where y(t) is the output of a single degree of freedom oscillator.

PY is a very simple quantity to measure. Unfortunately it is poorly correlated with damage. It is now well known that the behavior of a structure under earthquake loading depends not only on the amplitude of the ground motion, but also on its frequency content and duration [Refs 9, 11, 12]. Despite this, peak ground motion values, particularly PGA, continue to play a significant role in engineering design.

## 1.3. Effective Ground Motion

Since peak ground motion does not correlate well with structural response or damage, attempts have been made to define an 'effective' ground motion as some fraction of the peak value.

One such definition was given by Newmark and Hall during the course of several special design studies [Ref 2, p 25].

> [Effective acceleration] is that acceleration which is most closely related to structural response and to damage potential of an earthquake. It differs from and is less than the peak free-field ground acceleration. It is a function of the size of the loaded area, the frequency content of the excitation, which in turn depends on the closeness to the source of the earthquake, and to the weight, embedment, damping characteristic and stiffness of the structure and its foundation.

Although not precise, the significant aspect of this definition is that it relates structural response to the characteristics of the ground motion (frequency content, duration) and to the geometry and size of the structure.

## 1.4. Duration and RMS Acceleration

Bolt [Ref 13] defined duration of strong ground motion to be the elapsed time between the first and last excursions of a chosen level of ground acceleration (say 0.05 g, where g is the acceleration due to gravity). This has come to be known as the bracketed duration. Another definition, due to Trifunac and Brady [Ref 14], is based on the time during which 90% of the total energy of the ground motion has occurred. The energy is measured by integrals of the type

$$I(t) = \int_0^t a^2(\tau)d\tau \tag{B.2}$$

where t is some portion of the total time of the recording of the accelerogram a. Figure 5 shows the variation of I(t) with time for the Kern County accelerogram shown in Figure 3. The duration of strong ground motion beings at $t_1$ when 5% of the total energy has arrived and ends at $t_2$ when 95% has arrived.

Vanmarcke and Lai [Refs 15, 16] devised a more complicated definition of duration based on the root mean square acceleration.

$$RMSA = \left[\frac{1}{T}\int_0^T a^2(t)dt\right]^{\frac{1}{2}} \tag{B.3}$$

where a(t) is the accelerogram and T is the total duration of the record. Using the theory of stationary Gaussian random functions, a relationship between RMSA and PGA was established involving a duration during which the ratio PGA/RMSA is exceeded once on the average. The main advantages of this definition of duration are that it links duration with PGA and RMSA and that the underlying theory may be used to derive spectral representations (including response spectra) of ground motion based on duration for use in structural

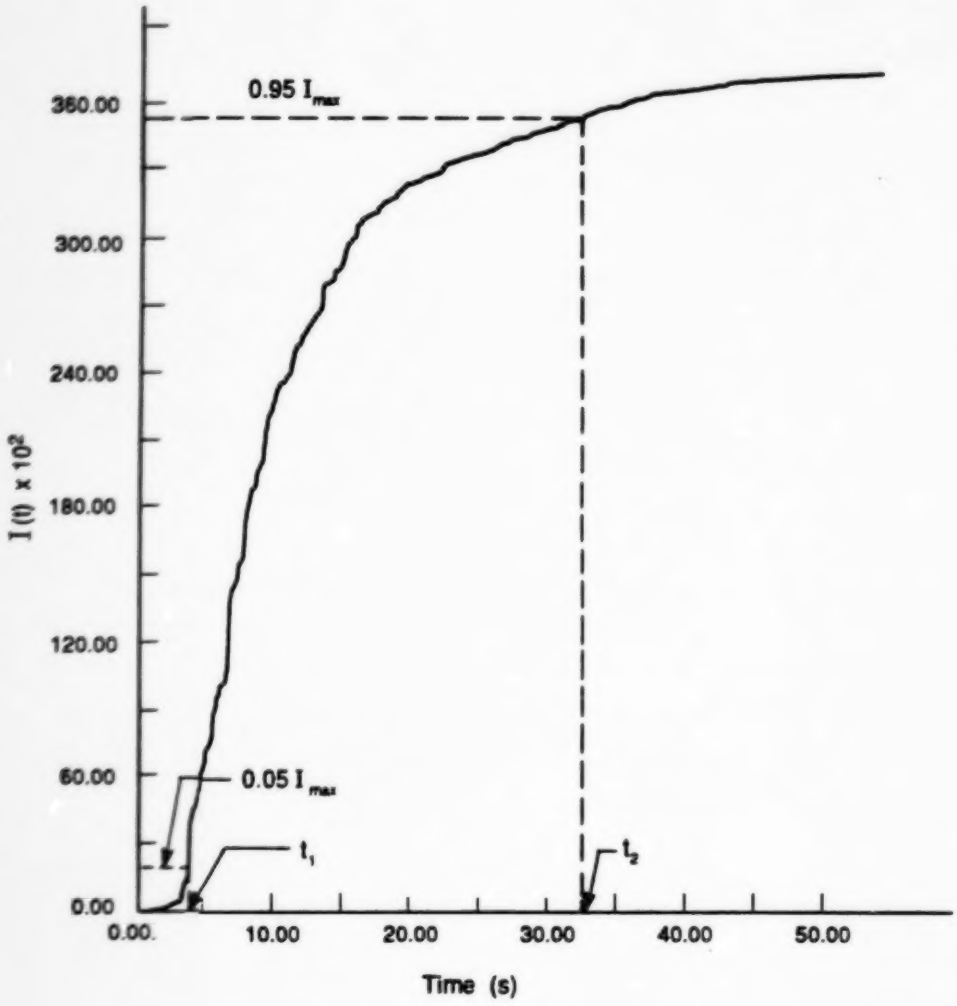


Fig. 5

Atomic Energy Control Board
The Effect of High Frequency Ground Motion on the Maple-X10 Reactor
I (t) of Kern County Accelerogram

ACRES

response analysis. However, the application of such an approach to structural analysis was not found in the literature.

McCann and Shah [Ref 17] used the variation of RMSA with time as a means of determining duration. For an accelerogram, a(t), the cumulative RMS ground motion is defined by

$$CRMS(t) = \left[\frac{1}{t}\int_0^t a^2(\tau)d\tau\right]^{\frac{1}{2}} \qquad (B.4)$$

In general CRMS increases to a maximum and then decays slowly to a final value. Initially the slope of CRMS is positive and large peaks occur corresponding to the arrivals of seismic waves causing strong ground motion. At later times the derivative becomes negative and remains so until the end of the record. Duration is defined as the elapsed time between the last occurrence of a negative derivative toward the beginning of the record and the last occurrence of a positive derivative toward the end of the record. This definition of duration is perhaps the most physically based since the CRMS function is a representation of the average rate of energy arrival as a function of time. However, determination of the derivative of CRMS can be a numerically unstable procedure.

Given a time interval $[t_1, t_2]$ during which strong ground motion is arriving, it becomes possible to define other measures of ground motion which could be termed effective ground motion. For example, the root mean square acceleration, Equation B.3 could be redefined as

$$RMSA = \left[\frac{1}{t_2 - t_1}\int_{t_1}^{t_2} a^2(t)dt\right]^{\frac{1}{2}} \qquad (B.5)$$

This is the definition used in Table 1-2. McCann and Shah [Ref 17] and others have found this to be a more robust measure of the intensity of earthquake motion.

Duration itself may be used as an indicator of damage. The response of lightly damped linear and nonlinear systems is known to depend on the duration of shaking. The occurrence of low-cycle fatigue (see Section 2.3) is also dependent on duration. However, the actual response depends on the type of structure and thus any measure of damage

involving duration is only meaningful in a comparative sense. An absolute measure of damage involving duration would require calibration using damage reports and analyses from past earthquakes. In addition, it has been suggested that, at least in the near-field, a more physical measure of duration would take fault rupture time into account [Ref 42].

## 1.5. Arias Intensity

The integral in Equation B.2 is a measure of the total energy available per unit mass of a single degree of freedom oscillator. This is known as the Arias intensity [Ref 9] and may also be used to assess damage potential in a comparative sense.

## 1.6. Cumulative Absolute Velocity

As a result of several incidents in the US where nuclear power plant operating limits were exceeded, but no damage was experienced, the Electric Power Research Institute commissioned a study [Ref 6] to develop a more reliable and meaningful criterion for exceedance of operating limits.

The current criterion in the US for exceedance of the operating limits is exceedance of the response spectrum of the operating basis earthquake (OBE). Specifically, the ordinates of the response spectrum of the OBE must be exceeded by the ordinates of response spectrum of the measured motion. Accelerograms and equipment capable of measuring response spectra directly are installed in most nuclear plants in the US (see Ref 18).

The problems with this criterion are many. Firstly, the methodology of selecting the OBE spectrum is not standardized. Secondly, a wide variety of instrumentation quality and data processing capability exists in all plants. Thirdly, exceedance is not defined precisely, and the frequencies at which exceedance is to be tested are not specified.

The advantages of using a response spectrum as a criterion lie mainly in its ease of measurement and that there is a relationship between the oscillator used to define the spectrum and the structure in question. However, a response spectral ordinate is a peak value, in a similar fashion to PGA, is likely poorly correlated with damage.

The EPRI study [Ref 6] focused on finding an alternative measure of damage that satisfied the following criteria.

(1) It would be related to actual damage observed in existing structures which had experienced earthquakes or blasts.

(2) It would be relatively easy to measure.

A measure found to satisfy the above criteria is the Cumulative Absolute Velocity (CAV)

$$CAV = \int_0^T |a(t)|dt \tag{B.6}$$

where a(t) is the accelerogram and T is the total duration of the record. Using damage records from blasts and earthquakes, it was found that if CAV exceeded 0.3 g-sec then a potentially damaging earthquake had occurred and the nuclear plant should be shut down for inspection (g is the acceleration due to gravity).

Note that the definition of the CAV takes account of both the amplitude and the duration of the record, thus taking account of the energy available in the ground motion. In fact, another interpretation of CAV is as follows: by sorting the values of acceleration in an accelerogram into descending order, the result is an acceleration exceedance curve which begins at coordinates (0, PGA) and ends at coordinates (T, 0) where T is the record length. CAV is the area under this curve. Figure 6 shows the exceedance curve for the Kern County accelerogram shown in Figure 3.

The use of CAV as an absolute damage criterion requires calibration using existing damage records. This was the main topic of the EPRI report [Ref 6]. The conclusion that a CAV exceeding 0.3 g-sec is an indication of damage is still under review.

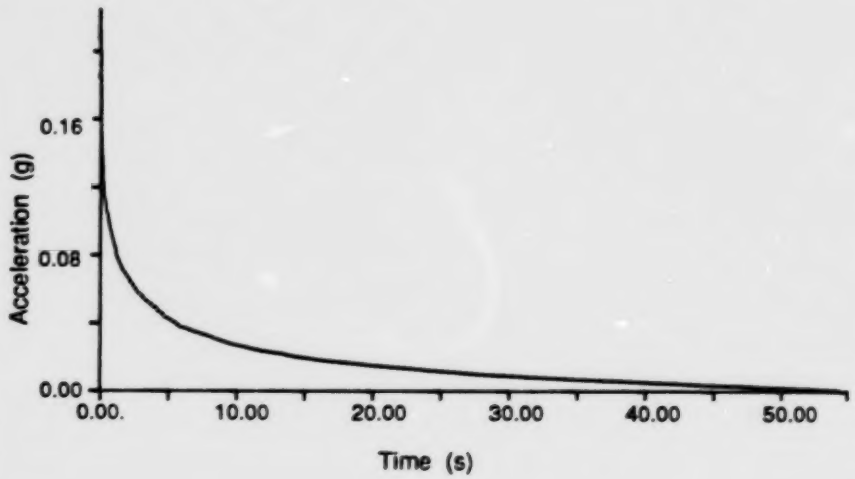


Fig. 6

Atomic Energy Control Board
The Effect of High Frequency Ground Motion on the Maple-X10 Reactor
Exceedance Curve of Kern County Accelerogram

ACRES

# 2. Damage Measures for Structural Models

Just as with measures of damage potential to structures, there is no unique way to measure the damage to a structural model. This is due, in part, to different perceptions of what causes damage in structures. However, all the measures to be discussed are physically based and often rely on extensive experimental data.

An extensive review of damage measures for structural models is given in Ref 19.

## 2.1. Maximum Allowable Stress or Deformation

Older building codes (circa 1940) required structures to be designed to withstand a specified maximum value of stress or deformation caused by ground motion. The causative force was assumed to act at the center of Figure 6 gravity of the structure and to have a magnitude given by the product of the weight of the structure and a seismic base shear coefficient. The base shear coefficient was larger in regions where large earthquakes were likely.

A similar approach is practiced today in building design as outlined in various building codes. The stresses or deformations in a structural model are computed and compared with allowable stresses (usually yield stresses) or deformations. If the latter are exceeded, then the design is adjusted to limit stresses and deformation within allowable limits. However, if the model is linear elastic, this approach neglects the ability of structural ductility to absorb energy.

Despite the limitations mentioned above, the use of the exceedance of a maximum allowable stress or deformation as a damage indicator for an elastic model is a simple procedure and useful for preliminary or comparative damage estimates. Examples of the application of this approach are given in Refs 20 and 21. An interesting example of a nonlinear analysis of a reactor structure is given in Ref 22. In this particular example, it was found that a linear elastic analysis indicated that maximum allowable stresses and deformations were exceeded. However, an inelastic analysis incorporating stiffness degradation predicted only one cycle of inelastic behavior, and therefore that failure would be unlikely.

## 2.2. Displacement Ductility

Later building codes recognized that considerable energy absorption capability existed in most structures and allowed a reduction in the design force (or stress or deformation) depending on the type of structure. Nonlinear behavior is incorporated into a linear analysis by the use of modified response spectra which account for the energy absorption capability by reducing the design response spectral ordinates. The current National Building Code of Canada provides a table [Ref 23, Table 4.1.9B, pp 168-169] of the allowable reduction factors. In order to use any one of these reduction factors, the structure must be of a type corresponding to the reduction factor and it must be designed with sufficient ductility to deform beyond the yield point without major structural failure. (Procedures for incorporating ductility in concrete and steel are outlined in CSA Standards CAN3-A23.3-M84 and CAN3-S16.1-M84, respectively.)

These ideas have been used to develop a damage measure for a structural model. The displacement ductility ratio is defined by

$$\mu = \frac{u_m}{u_y}$$

where $u_m$ is the maximum displacement at a point in the structure and $u_y$ is the yield displacement. Then, assuming the materials in the structural model are capable of withstanding a displacement $u_m$, any displacement greater than $u_m$ would be indicative of damage. One problem with this approach is that $\mu$ must be defined for the structural model (any value between 2 and 6 might be reasonable). A more serious limitation is that cumulative damage caused by repeated exceedances of the yield displacement is not accounted for.

In regard to the effect of high-frequency ground motion on ductile reactor type structures with low-frequency (<10 Hz) modes, calculations described in Ref 6 provide some interesting comparisons. In these analyses a 7% damped nonlinear single degree of freedom of oscillator was designed to yield (i.e., result in a ductility ratio of unity) at the spectral accelerations of the US NRC Regulatory Guide 1.60 response spectrum anchored to a PGA of 0.2 g. The oscillator was then subjected to a total of 39 accelerograms, 16 of

which resulted from ENA earthquakes and exhibited high-frequency motion and 23 of which resulted from WNA earthquakes and exhibited low-frequency motion.

In Ref 6 an artificial time history was generated to match the NRC Regulatory Guide 1.60 response spectrum. The response to this time history may be assumed typical of that of the WNA accelerograms. Four of the 16 ENA accelerograms quoted in Table 4-4 of Ref 6 were selected as typical of ENA ground motion. The amplifications required of these four accelerograms over that required of the WNA accelerogram to achieve a given ductility ratio are shown in Table 2.

From Table 2 it may be seen that for low-frequency oscillators, the amplitudes of the four ENA accelerograms have to be higher, by a factor of 2 or more, relative to a typical WNA accelerogram in order to achieve a given ductility ratio. Thus, based on this ductility ratio criterion, these high-frequency ground motions would be less damaging to typical low-natural frequency components in a nuclear power plant.

At high oscillator frequencies it is difficult to distinguish damage potential of ENA and WNA ground motion based on ductility. However, the displacements at these frequencies were found to be too small to cause damage to ductile components. It was concluded in Ref 6 that a damage measure based on a ductility limit which increases with frequency would be more realistic.

Further discussion of displacement ductility may be found in Refs 2, 24, 25, 26, 27 and 28, and in Commentary J of Ref 23.

## 2.3. Cumulative Damage and and Fatigue Failure Mechanisms

Large-scale experimental tests of structural members have demonstrated the importance of cumulative effects leading to damage or failure. Such effects can lead to material degradation which naturally affects the strength and energy dissipation capability of the structure. Several theoretical studies of such behavior have been done for single degree of freedom oscillators [Refs 37, 38] and for steel and reinforced concrete structures [Refs 39 and 40]. The results indicate responses that are considerably different from those predicted

## TABLE 2

## AMPLIFICATION REQUIRED OF ENA ACCELEROGRAMS TO ACHIEVE A GIVEN DUCTILITY RATIO

(From Table 4-4 of Ref 6)

Ductility Ratio 1.00

| | Frequency (Hz) | | | | | |
|---|---|---|---|---|---|---|
| Record No.† | 5.34 | 8.54 | 11.00 | 15.00 | 20.00 | 23.00 |
| 4 | 1.00 | 1.00 | 1.00 | 1.00 | 1.00 | 1.00 |
| 18 | 3.95 | 2.80 | 1.75 | 1.10 | 0.50 | 0.50 |
| 19 | 4.25 | 3.70 | 2.70 | 1.25 | 0.45 | 0.35 |
| 25 | 11.40 | 3.35 | 0.95 | 0.55 | 0.60 | 0.60 |
| 35 | 12.75 | 3.30 | 1.35 | 1.25 | 0.80 | 0.40 |

Ductility Ratio 1.85

| | Frequency (Hz) | | | | | |
|---|---|---|---|---|---|---|
| Record No.† | 5.34 | 8.54 | 11.00 | 15.00 | 20.00 | 23.00 |
| 4 | 1.00 | 1.00 | 1.00 | 1.00 | 1.00 | 1.00 |
| 18 | 4.73 | 3.13 | 1.81 | 1.37 | 0.78 | 0.58 |
| 19 | 4.83 | 3.65 | 3.37 | 2.26 | 0.56 | 0.54 |
| 25 | 15.34 | 4.29 | 1.93 | 0.67 | 0.74 | 0.73 |
| 35 | 12.66 | 3.68 | 2.19 | 1.30 | 1.00 | 0.77 |

Ductility Ratio 4.27

| | Frequency (Hz) | | | | | |
|---|---|---|---|---|---|---|
| Record No.† | 5.34 | 8.54 | 11.00 | 15.00 | 20.00 | 23.00 |
| 4 | 1.00 | 1.00 | 1.00 | 1.00 | 1.00 | 1.00 |
| 18 | 12.14 | 4.08 | 3.31 | 1.84 | 1.41 | 1.07 |
| 19 | 6.00 | 4.70 | 3.89 | 3.06 | 1.90 | 0.87 |
| 25 | 19.05 | 9.28 | 4.75 | 1.81 | 0.93 | 0.90 |
| 35 | 24.21 | 10.13 | 3.86 | 2.25 | 1.52 | 1.17 |

† Record No. 4 is an artificial time history generated to match the NRC Regulatory Guide 1.60 response spectrum; it is representative of a WNA type accelerogram. Record Nos. 18, 19, 25 and 35 are actual ENA accelerograms.

by assuming elastic or ideal plastic behavior. In Ref 40 levels of damage were found to be a strong function of model ductility and duration of strong ground motion.

Permitting inelastic response during earthquakes admits the possibility of low cycle fatigue during an earthquake. Analyses of this type of failure on single degree of freedom structures are discussed in Refs 29, 30 and 31. However, low cycle fatigue is a rather special kind of failure mechanism usually confined to small localized areas of a structure (e.g., bolt holes, welds, etc). Generally, structural design would tend to minimize the possibility of fatigue failure due to earthquakes. Owing to this and that the earthquakes of interest have relatively short durations and few cycles, fatigue failure was not considered in this study.

## 2.4. Energy Absorption and Dissipation

Energy input to a structure subjected to earthquake ground motion is dissipated by both damping and/or inelastic deformation. If the structure is designed to withstand the inelastic deformation, then the stored energy (i.e., the energy that is not dissipated) is available to do damage. The amount and character of stored energy during an earthquake may therefore be used as an indicator of damage.

Derivations of equations for the energy partitioning in a linear single degree of freedom structure are given in Appendix A. Whether linear or nonlinear behavior is included in a structural model, the following equation applies at any time during the ground motion.

$$E_s = E_k + E_p = E_i - E_d$$

where $E_s$ is the stored energy composed of both kinetic energy, $E_k$, and potential energy, $E_p$. The energy input by the ground motion is $E_i$ and the energy dissipated by viscous damping is $E_d$. Nonlinear behavior would be included in the potential (or strain) energy term, $E_p$.

The use of energy absorption and dissipation offers a physically based means of assessing the damage to a structural model. For example, in Refs 32 and 33, it was shown that the response parameters that affect damage were the amount of energy input and the amount

of energy dissipated by hysteretic behavior and damping. The number of yield excursions and reversals was suggested as a measure of structural damage. Based on this, it was shown that longer duration ground motion caused more yield excursions in a single degree of freedom oscillator than short-duration motion. Similar conclusions were found in Ref 34.

The use of energy partitioning and/or yield reversals as a measure of damage in a structural model naturally depends on the characteristics of the model. Thus, these damage measures are not absolute and must be confined to particular well-defined structural types or calibrated in some way in order to be useful.

## 2.5. Empirical Damage Measures

Blast damage reports have been used to define criteria for predicting blast damage to structures. Although the character of ground motion due to a nearby blast is different from that due to a near-field (say within 10 km) moderate magnitude earthquake, the amplitudes may be similar. In the high-frequency range (>10 Hz), the response spectral ordinates of the ground motion due to surface mine and quarry blasts are comparable to those of the near-field selected accelerograms, as shown in Figure 7. In addition, although the energy content is much lower, blasts produce ground motion with frequencies in the 10 - 100 Hz range. Thus, in this sense, blast damage criteria may be used as a damage measure in the high-frequency range.

The most highly developed criterion for blast damage is due to Dowding [Ref 35]. Using ground motions due to blasts and associated damage reports to basement walls given by Edwards and Northwood [Ref 36], Dowding developed 'no-cracking' response spectral bounds which enveloped all cases of no observed cracking in basement walls. The result is shown in Figure 8.

Application of a no-damage criterion for basement walls composed of low-strength concrete may seem conservative for structures such as composed of higher strength concrete. It would seem that the bounds should be higher. However, as pointed out in Ref 6, a basement wall is an embedded structure and amplification of motion would occur in an above-ground structure. Thus, pending further verification, the bounds shown in Figure 8

are probably suitable for above-ground concrete structures. The significant aspect of this criterion is the large allowable accelerations in the high-frequency range.

Machine vibration and equipment fragility test data have also been used to infer whether high-frequency ground motion is damaging to structures and equipment [Ref 6]. The basic conclusion from these data is that damage due to high-frequency motion is extremely unlikely. It should be noted that the use of such data to establish a criterion for structures would be conservative since the motions to which the machines and equipment are subjected are of longer duration and higher frequency content than the motion due to earthquakes.

## 3. Discussion

It is apparent that there is no unique measure of the damage potential of an earthquake or of the damage to a structural model due to a given ground motion. However, a meaningful measure of damage potential must take amplitude, amplitude distribution, duration and frequency content (or, equivalently, the energy content) of the ground motion into account. In addition, a meaningful measure of structural model damage must account for the ability of the motion to cause significant inelastic behavior and cumulative damage, a phenomenon related to the characteristics of both the structural model and the ground motion.

Any numerical measure of damage potential or damage to a structural model is a relative one. Calibration with existing damage records or by means of testing is necessary to establish an absolute measure of damage.

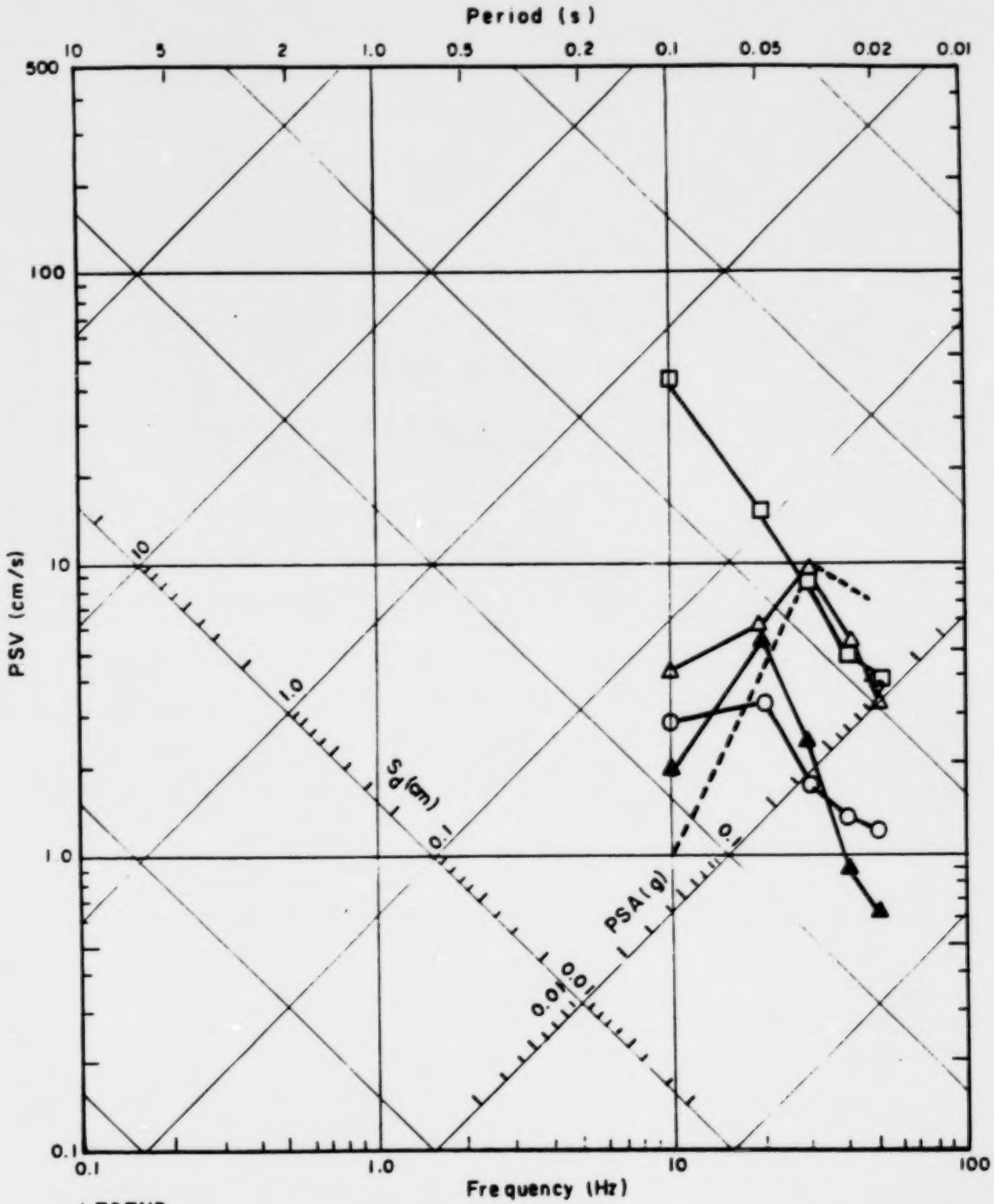


Fig. 7

Atomic Energy Control Board
The Effect of High Frequency Ground Motion on the Maple-X10 Reactor
ENA Response Spectra Versus Quarry Blast Spectrum (3% Damping)

ACRES

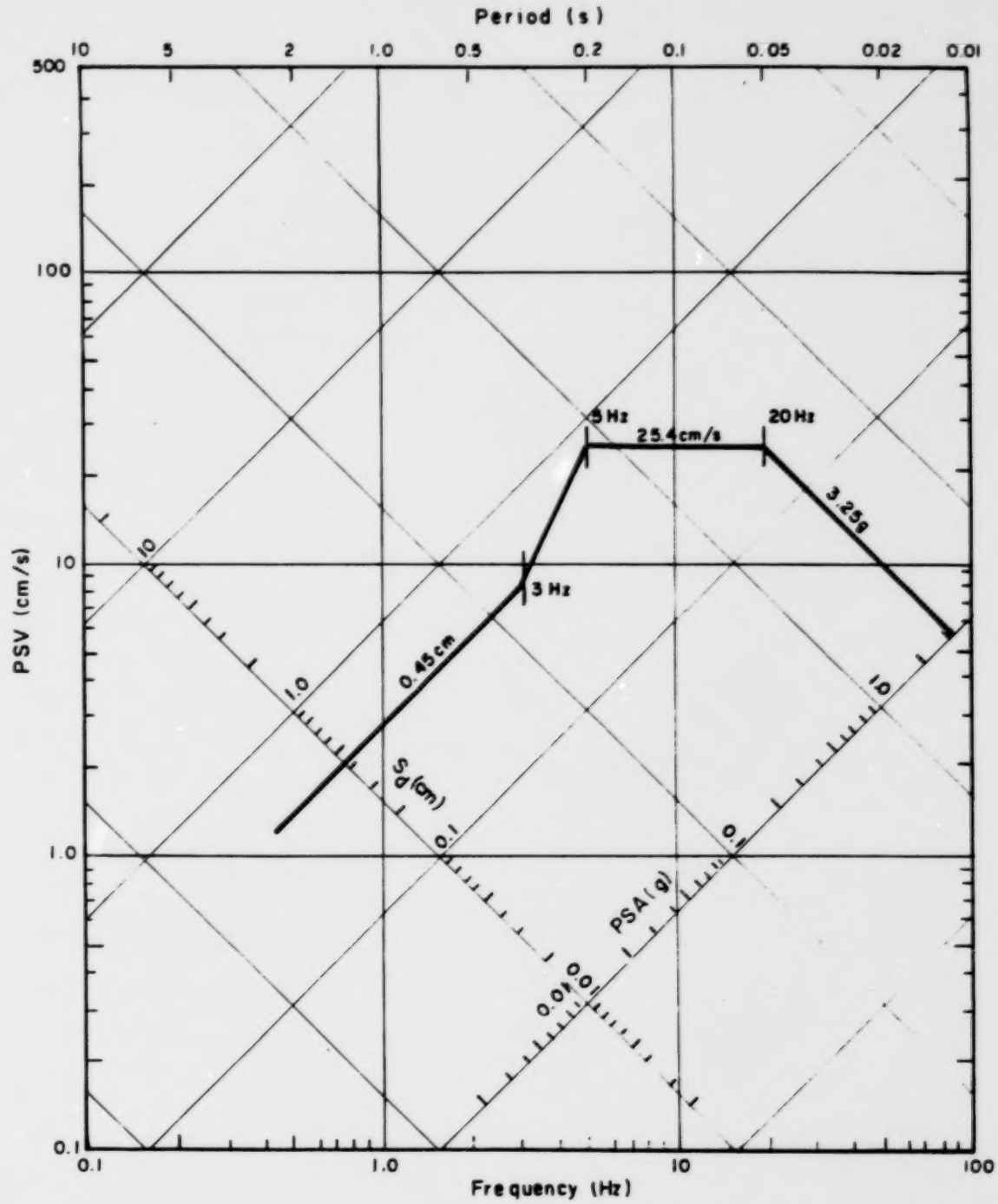


AFTER REF 35

Fig. 8

Atomic Energy Control Board
The Effect of High Frequency Ground Motion on the Maple-X10 Reactor
Blast Damage Threshold Criterion (3% Damping)

ACRES

# C. Analyses of Model Structures

## 1. SDOF Models

An analysis of the single degree of freedom model will illustrate the basic ideas and implications of the use of the response spectrum for the design of structures with high natural frequencies. Although the model is linear, it will be possible to infer much about the behavior of structures with high natural frequencies subjected to high-frequency ground motion.

### 1.1. Response Spectra

Examination of the response spectra in Figures 4-1 and 4-2 shows that accelerations (i.e., forces) are relatively large in the high-frequency (>10 Hz) portion of the spectrum. This is particularly true of the ENA earthquakes Leroy, Ohio, Miramichi, Nahanni and, to a lesser extent, Saguenay. However, displacements are much lower than those in the low frequency end of the spectrum.

At high oscillator frequencies, relative to the dominant frequencies of the ground motion, the peak response of the mass tends to be some multiple of the peak ground acceleration until finally, when the oscillator frequency is very high relative to the frequencies of the ground motion, the peak response is equal to the peak ground acceleration (see Appendix A). For earthquakes in WNA the peak response is equal to the peak ground acceleration at frequencies greater than 33 Hz (see Refs 2, 3). However, by comparing the peak response at high frequencies with the peak ground accelerations in Table 1-2, it appears that for earthquakes in ENA the corresponding upper frequency bound seems to be much higher than 33 Hz. Owing to the difference between the recorded frequency content of the selected WNA accelerograms and ENA accelerograms (see Chapter A, 1 and Table 1-2), the comparison of peak response is only fair at frequencies in the 10-25 Hz range. Despite this, the difference in the response spectra at higher frequencies is significant.

The option of scaling the accelerograms to some common value of PGA in order to make a fair comparison between the response spectra was examined. Scaling changes the magnitude of the difference between the response to ENA and WNA accelerograms in the high-frequency portion of the spectrum. For example, the response spectra resulting from scaling the selected accelerograms to a PGA of 0.2 g are shown in Figure 9. (Since the SDOF model is linear, the response of the ith scaled accelerogram is given by multiplying its original spectral ordinates by $0.2/PGA_i$.) The conclusion that the response spectra of ENA accelerograms are higher than those of WNA accelerograms in the high-frequency range is still valid. This is believed to be the significant aspect of the difference between ENA and WNA ground motion and, based on the four ENA accelerograms selected, appears to be independent of earthquake magnitude, epicentral distance or PGA. In other words, differences between ENA and WNA ground motion due to frequency are already demonstrated in the unscaled response spectra (see discussion in Appendix A).

The change in magnitude of the response may be deceptive since it depends on the PGA chosen to scale the accelerograms. Also, from a seismological point of view, the correlation between PGA and earthquake magnitude, particularly at short epicentral distances, is poor (e.g., compare the PGA of Parkfield with that of Nahanni, Table 1-2). In addition, there is no apparent relationship between PGA and the other amplitudes in an accelerogram, and the shape of the response spectrum is known to change with magnitude and epicentral distance (see Appendix A). For these reasons, it is recommended that comparisons between response be made on a statistical basis.

## 1.2. Energy Spectra

The energy stored in a structure as a result of being subjected to ground motion was discussed in Chapter B, 2.4. Further mathematical details are given in Appendix A. Basically, the stored energy is the energy available to do damage to a structure.

Stored energy varies with time much like other types of oscillator response. An energy spectrum is a plot of the peak value of stored energy versus oscillator frequency for a particular value of damping. This is similar to a response spectrum.

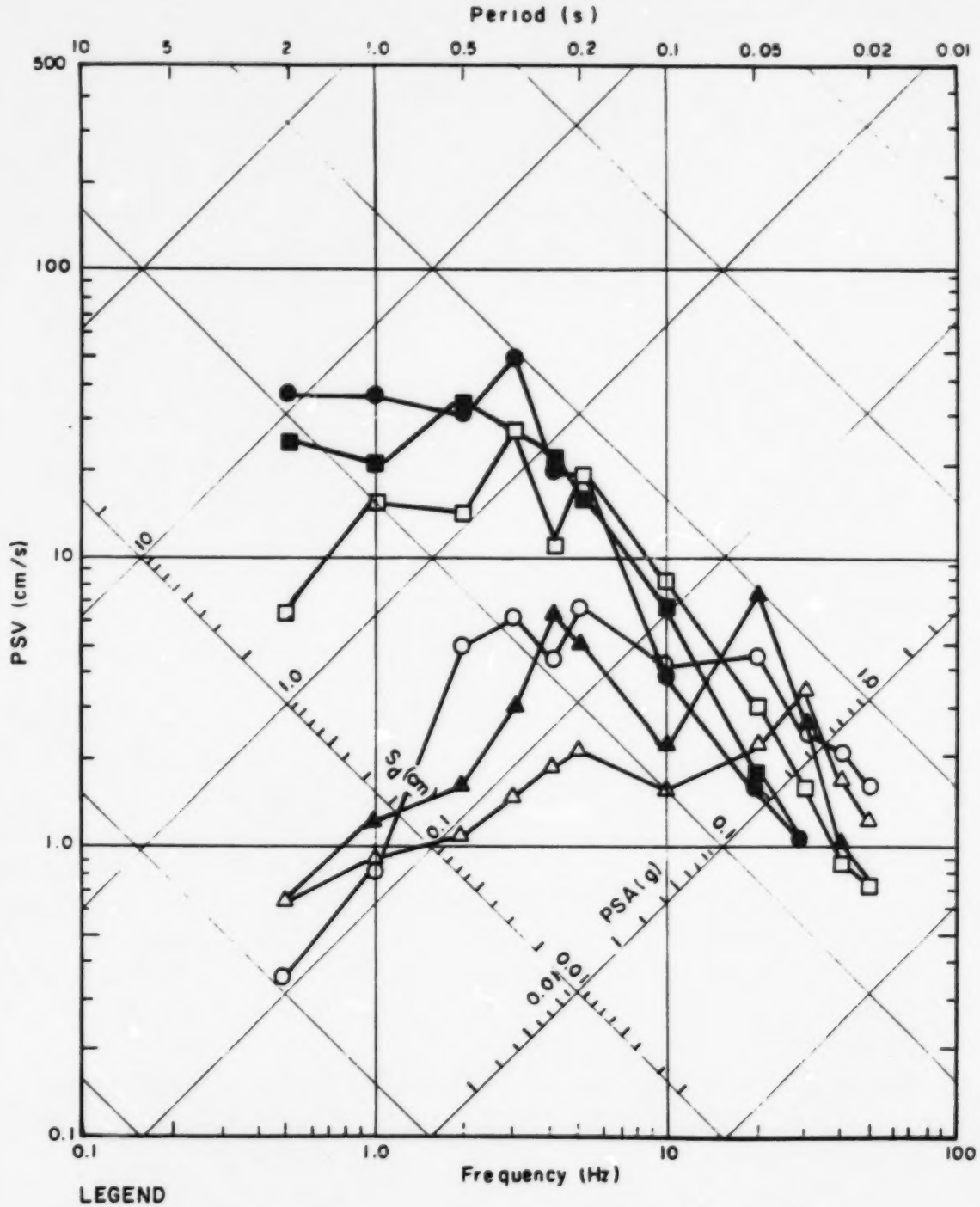


Fig. 9

Atomic Energy Control Board

The Effect of High Frequency Ground Motion on the Maple-X10 Reactor

Response Spectra of Scaled Selected Accelerograms (2% Damping)

ACRES

It would seem from the discussion in Chapter B that the character of the time variation of stored energy would be of interest. However, for purposes of comparison, the peak values are used. It turns out that these values are useful indicators of the effect of high-frequency ground motion. Energy spectra for the selected accelerograms are shown in Figure 10.

Although the sample is small (four earthquakes), it appears that high-frequency ground motion, such as the at recorded in ENA, results in a small amount of stored energy in low-natural frequency (<10 Hz) structures. Nahanni is an exception. This would explain the reason for the discrepancy between observed damage in low-natural frequency structures and predicted on the basis of peak motions.

At high-natural frequencies, there is no clear distinction in terms of stored energy between ENA and WNA ground motion. This may be due, in part, to the difference in recorded frequency content of the selected WNA and ENA accelerograms. A similar lack of clear distinction between the two types of ground motion was found in Chapter B, 2.2 in regard to amplifications required of ENA accelerograms to achieve certain ductility ratios.

## 1.3. Blast Damage Threshold Criterion

A more empirical demonstration of the discrepancy between observed and predicted damage may be had by plotting the 3% damped response spectra of the selected accelerograms and comparing them to the blast damage threshold spectrum shown in Figure 8. The result is shown in Figure 11. The spectra of all the selected accelerograms fall below the blast damage threshold at oscillator frequencies greater than 10 Hz. This indicates that none of the selected earthquakes can be expected to do significant structural damage in this frequency range.

The use of blast damage threshold criteria in comparison with the response spectra of recorded accelerograms forms part of an argument for ignoring structural response at natural frequencies greater than 10 Hz [Ref 6]. However, while exhibiting some similarities, ground motion due to blasts is generally different in both frequency and energy content from ground motion due to earthquakes. Also, the actual response depends on the structure in question.

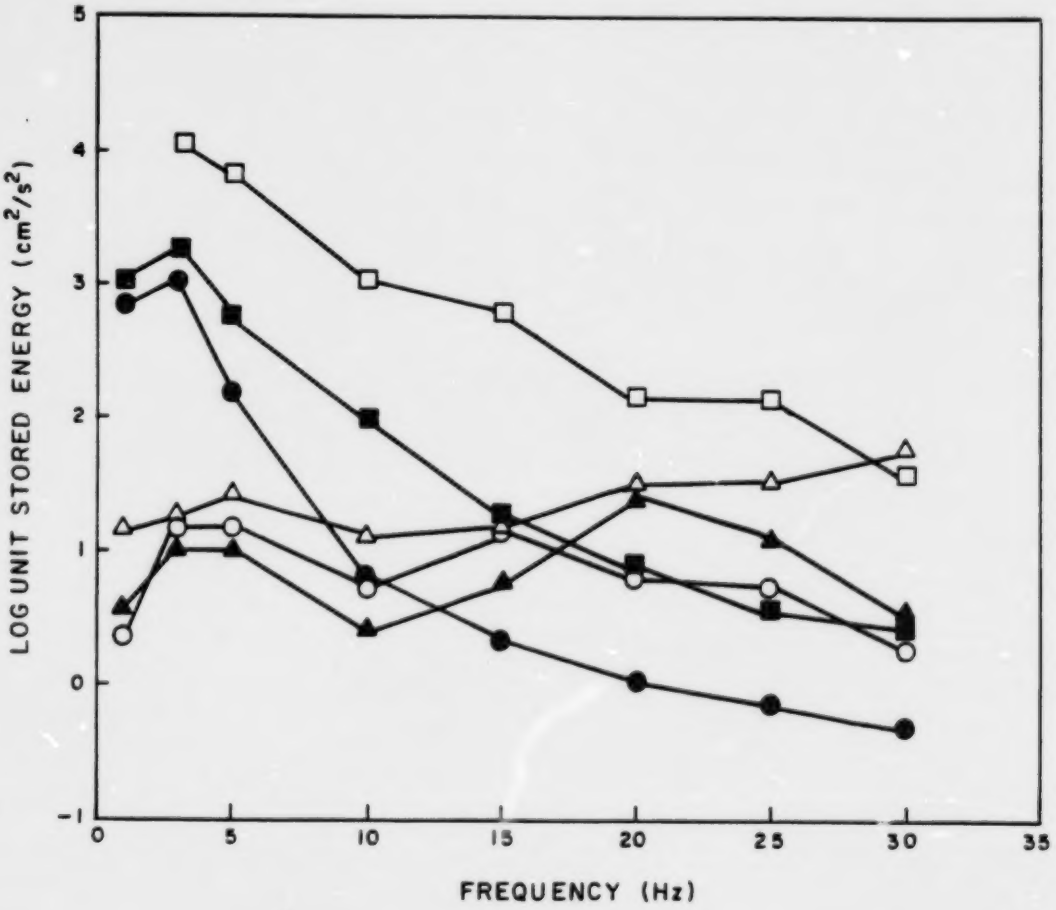


LEGEND

- ● KERN COUNTY
- ○ SAGUENAY
- ■ PARKFIELD
- □ NAHANNI
- ▲ LEROY, OHIO
- △ MIRAMICHI

Fig. 10

Atomic Energy Control Board
The Effect of High Frequency Ground Motion on the Maple-X10 Reactor
Energy Spectra of Selected Accelerograms (2% Damping)

ACRES

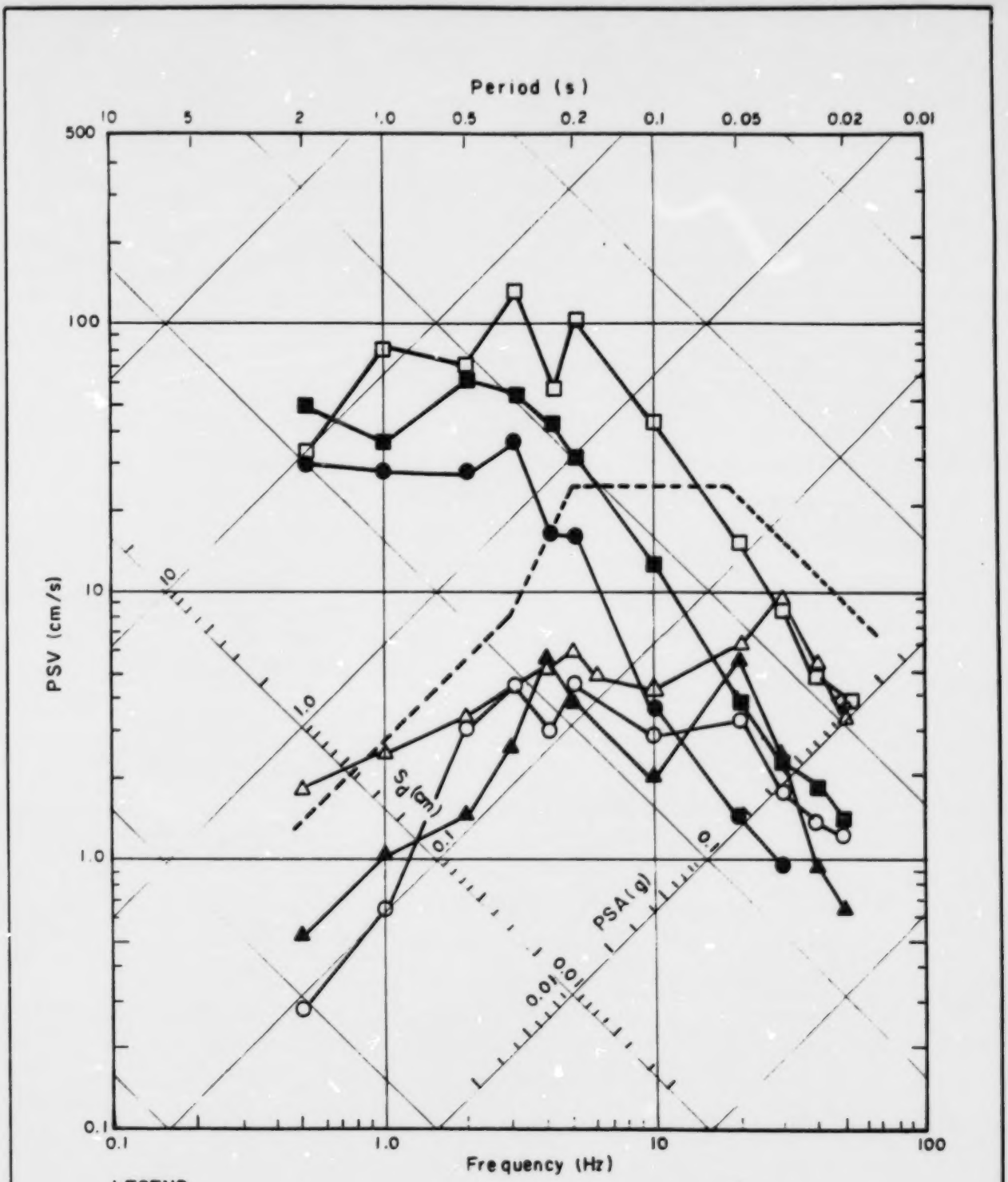


Fig. 11

Atomic Energy Control Board

The Effect of High Frequency Ground Motion on the Maple-X10 Reactor

Response Spectra Versus Blast Damage Threshold (3% Damping)

## 1.4. Discussion

The response of a SDOF oscillator to the selected accelerograms indicates that large forces would be produced in structures with high natural frequencies when subjected to high-frequency ENA style ground motion. However, the corresponding displacements produced by high-frequency ground motion are relatively small. In addition, the response spectra of the selected accelerograms all fall below a blast damage threshold at oscillator frequencies greater than 10 Hz.

Although a response spectrum may be a convenient indicator of damage potential in the low-frequency range (<10 Hz), the same may not be true in the high-frequency range. From the discussion, in Chapter B, 3, it is evident that amplitude, amplitude distribution, duration and frequency content all contribute to structural damage (or lack thereof). However, a response spectrum does not take these factors into account in a direct or unbiased manner. In fact, there exist many accelerograms (theoretically an infinite number) which could produce the same response spectral ordinate.

For example, the response spectral ordinate at 5% damping of the Leroy, Ohio accelerogram is 5.387 cm/s. A 20-Hz sinusoid of 10 seconds duration and amplitude 70 $cm/s^2$ would produce approximately the same spectral ordinate. However, using CAV as a damage indicator, the sinusoid would likely produce more damage. The CAV of the sinusoid is approximately 0.45 g-sec, whereas that of the Leroy, Ohio accelerogram is 0.085 g-sec, well below the 0.3 g-sec limit given in Ref 6. The first 5 seconds of the time histories of the velocity response of a 20-Hz oscillator to the sinusoid and to the Leroy, Ohio accelerogram are shown in Figure 12. Both longer and considerably shorter duration, 20-Hz sinusoids would produce the same spectral response as the Leroy, Ohio earthquake. Suitable combinations of sinusoids could be constructed to produce a match to the response spectra of the selected accelerograms over a range of frequencies, but the resulting time histories could possess an infinite variety of amplitude distributions, duration and frequency content.

Thus, in general, the response spectrum is not an indicator of the energy imparted to a structure and therefore the potential for damage. A response spectral ordinate is a peak quantity, the limitations of which were discussed in Chapter B, 1.2.

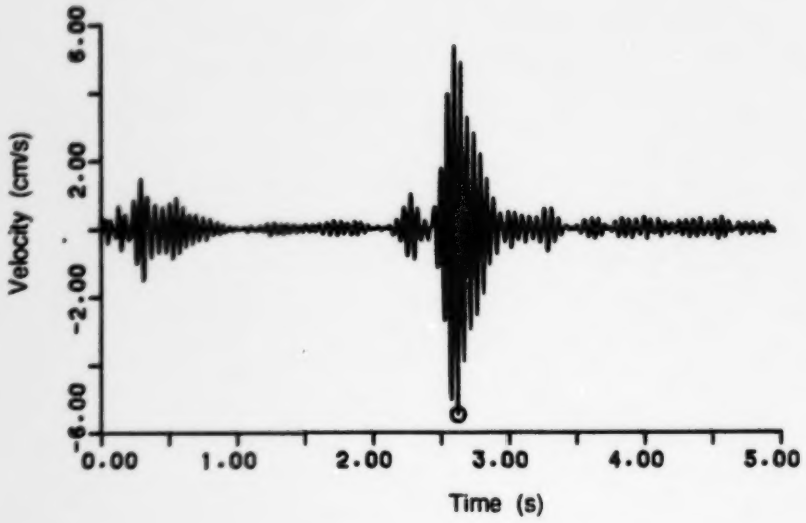


Response to Leroy, Ohio

O Peak Response
(Response Spectral Ordinate)
5% Damping

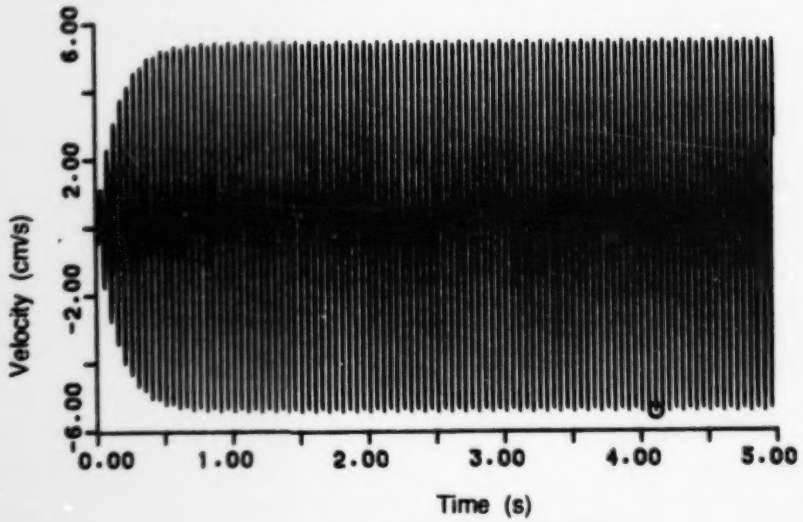


Response to Sinusoid

Fig.12

Atomic Energy Control Board
The Effect of High Frequency Ground Motion on the Maple-X10 Reactor
Velocity Response to Sinusoid and Leroy, Ohio Accelerogram

ACRES

Design by means of response spectra has worked so well in the low-frequency (1 - 10 Hz) range because strong ground motion in this frequency range is likely of longer duration than higher frequency strong ground motion. Longer duration ground motion is potentially more damaging in that more energy is available in such motion. Considerable uncertainty exists as to how this energy is dissipated in a structure and, in the face of such uncertainty, it makes sense to use a peak value for design. This is one reason most well-designed structures survive large, long-duration earthquakes. However, it is evident that application of the same approach in the high-frequency range could result in a conservative design, unless the response spectrum is modified to take actual high-frequency structural response into account.

## 2. MDOF Model

The analyses of the SDOF model served to illustrate some basic aspects of the effects of high-frequency ground motion on structures. Similar effects should be observed in a MDOF model, although the details and analysis of the results will differ. To confirm this, analyses of a simple MDOF column model with high-natural frequencies were performed. The model is the vertical steel column shown in Figure 13. The column was divided into six beam elements, each with a specified cross-sectional area and moment of inertia. It was desired that the frequencies of the first two modes of the model be less than 30 Hz. For this reason, an additional mass of 300 kg was added to Node 3. Table 3 lists the model parameters and modal frequencies. The model was subjected to the selected accelerograms of the base. Only the first three modes were used in the analyses; the other modes are at much higher frequency and the model response is essentially determined by the first three modes. All of the analyses were done by means of the SAP IV finite element code [Ref 41].

Figure 14 shows the maximum bending moments computed at Nodes 2, 4 and 6 of the model. Since Node 1 is fixed, the largest bending moments occur at Node 2. Figure 15 shows the maximum relative deflections at Nodes 3, 5 and 7. Relative deflection at the ith node is defined as $u_i$-$u_{i-2}$. The displacements increase toward the top of the beam.

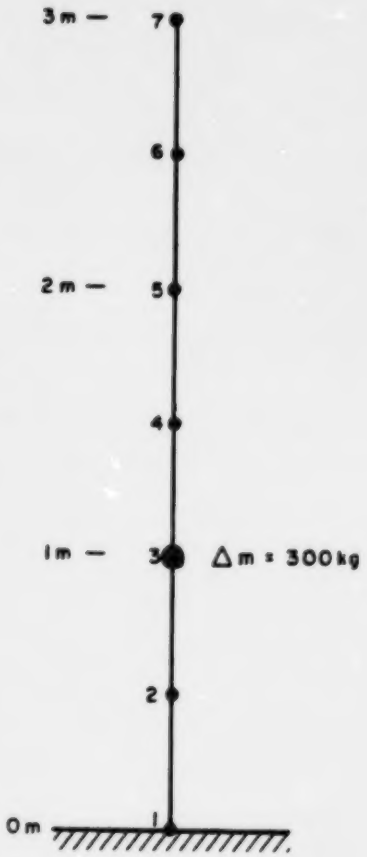


Fig. 13

Atomic Energy Control Board
The Effect of High Frequency Ground Motion on the Maple-X10 Reactor
MDOF Beam Model

ACRES

## TABLE 3

## MDOF MODEL PROPERTIES

### Material Properties

| | |
|---|---|
| Young's Modulus: | $2 \times 10^5$ MPa (steel) |
| Poisson's Ratio: | 0.3 |
| Density: | 7850 kg/m$^3$ |
| Yield Stress: | 275 Mpa |

### Geometric Properties

| | Height | | |
|---|---|---|---|
| | 0-1 m | 1-2 m | 2-3 m |
| Cross-sectional area (m$^2$) | $7.5 \times 10^{-4}$ | $2.0 \times 10^{-3}$ | $2.5 \times 10^{-4}$ |
| Moment of inertia (m$^4$) | $1.5 \times 10^{-7}$ | $3.0 \times 10^{-7}$ | $5.0 \times 10^{-6}$ |

### Natural Frequencies (Hz)

$f_1 = 18.2$
$f_2 = 29.1$
$f_3 = 97.0$

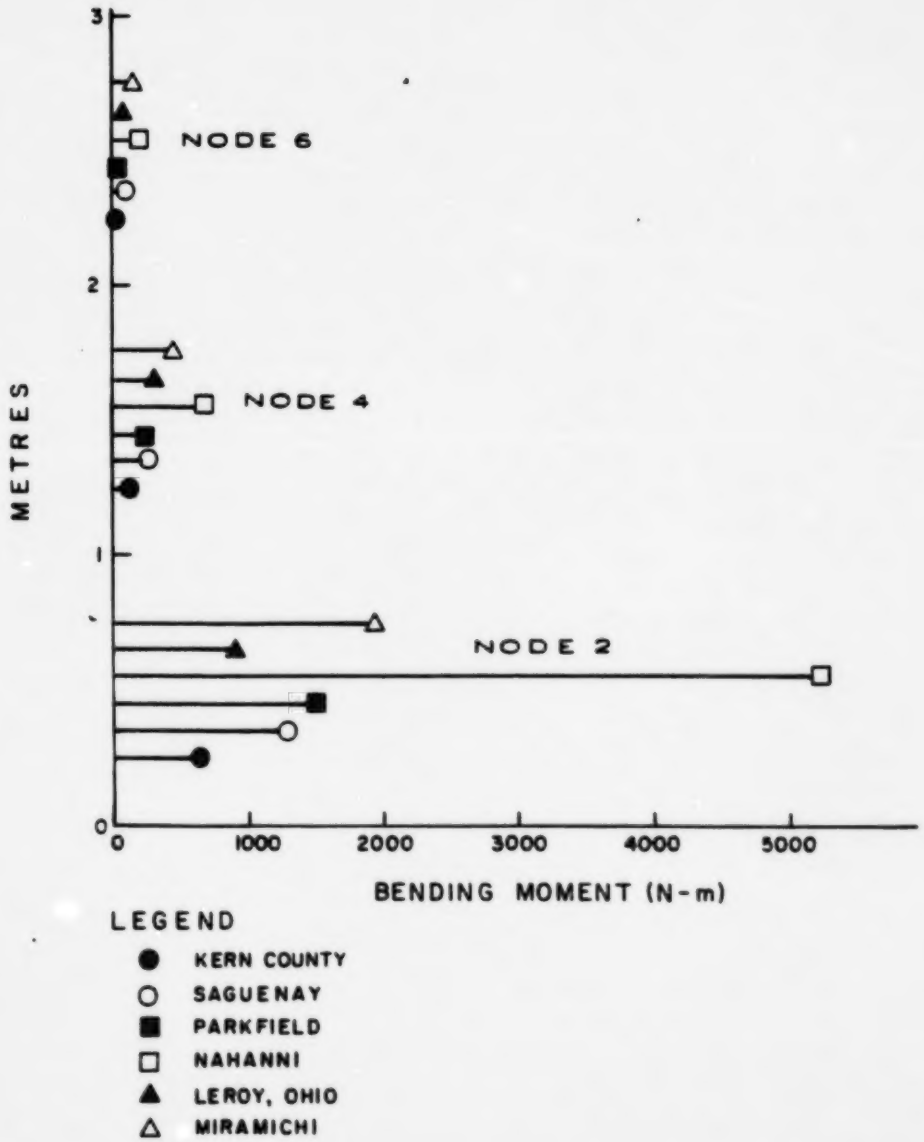


Fig. 14

Atomic Energy Control Board
The Effect of High Frequency Ground Motion on the Maple-X10 Reactor
Maximum Bending Moments of MDOF Model

ACRES

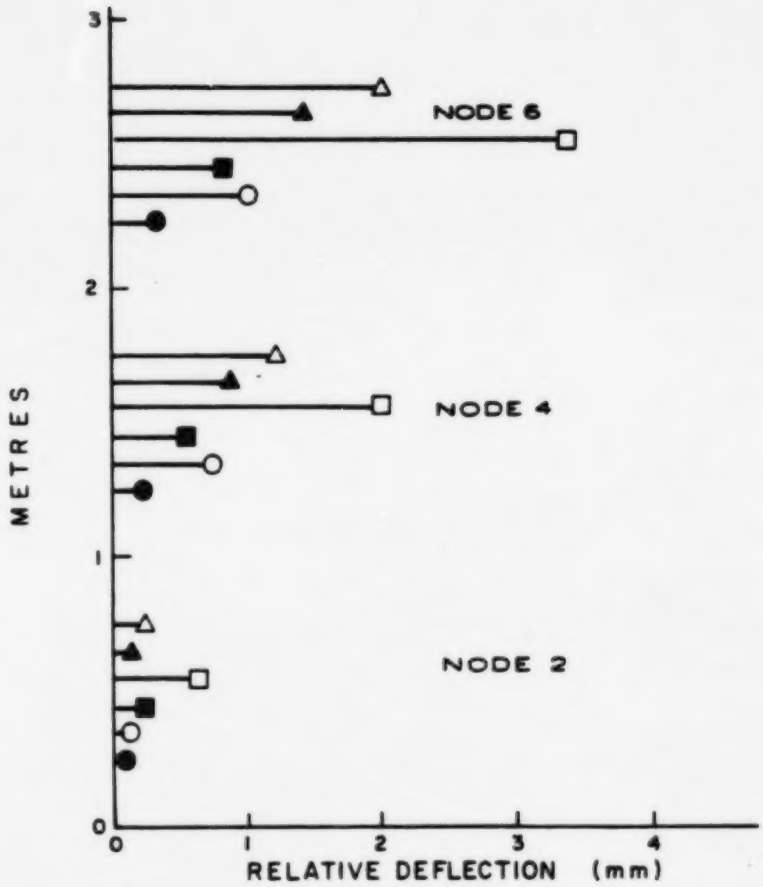


LEGEND

- KERN COUNTY
- SAGUENAY
- PARKFIELD
- NAHANNI
- LEROY, OHIO
- MIRAMICHI

Fig. 15

Atomic Energy Control Board
The Effect of High Frequency Ground Motion on the Maple-X10 Reactor
Maximum Relative Deflections of MDOF Model

The largest maximum displacements and bending moments in the beam are mostly induced by the ENA accelerograms. This is consistent with the response spectra of these accelerograms in the 10 - 30 Hz range. A more realistic assessment of the damage potential of these accelerograms may be made by sorting the bending moment time histories into descending order and thus determining the exceedance curve for bending moment. This is similar to the interpretation of the CAV damage potential measure discussed in Chapter B, 1.6.

The exceedance curves for bending moment at Node 2 are shown in Figure 16. In general, the exceedance time of the larger values of bending moment is short. Using the area under these curves as a relative measure of damage, it may be seen that, with the exception of Nahanni, the damage due to the ENA accelerograms is likely to be small. However, note that this depends on the value of a threshold bending moment selected. For example, if it could be established that a bending moment of 100 N-m or less could be tolerated, then the comparisons of areas under the exceedance curves above 100 N-m would result in a different conclusion as to the damage potential of a particular type of ground motion. This means that specific structures must be analyzed in detail to determine damage potential.

## 3. Implications for the Maple-X10 Reactor

The above analyses of linear SDOF and MDOF systems allow the following general statements concerning the response of the Maple-X10 reactor to high-frequency ground motion.

The Maple-X10 reactor will be housed in a steel frame building with the actual reactor located in a concrete structure founded on rock. These structures have low-natural frequencies and, based on the discussion in Chapter C, 1.2, would not be adversely affected by high-frequency ground motion.

The reactor itself consists of an inlet plenum which supports a large heavy water tank, the fuel assemblies and the piping for the coolant system. It is composed mainly of stainless steel and various alloys. The natural frequencies of this structure are reported to lie in the 15-30 Hz range. If subjected to high-frequency ground motion similar to that in the selected

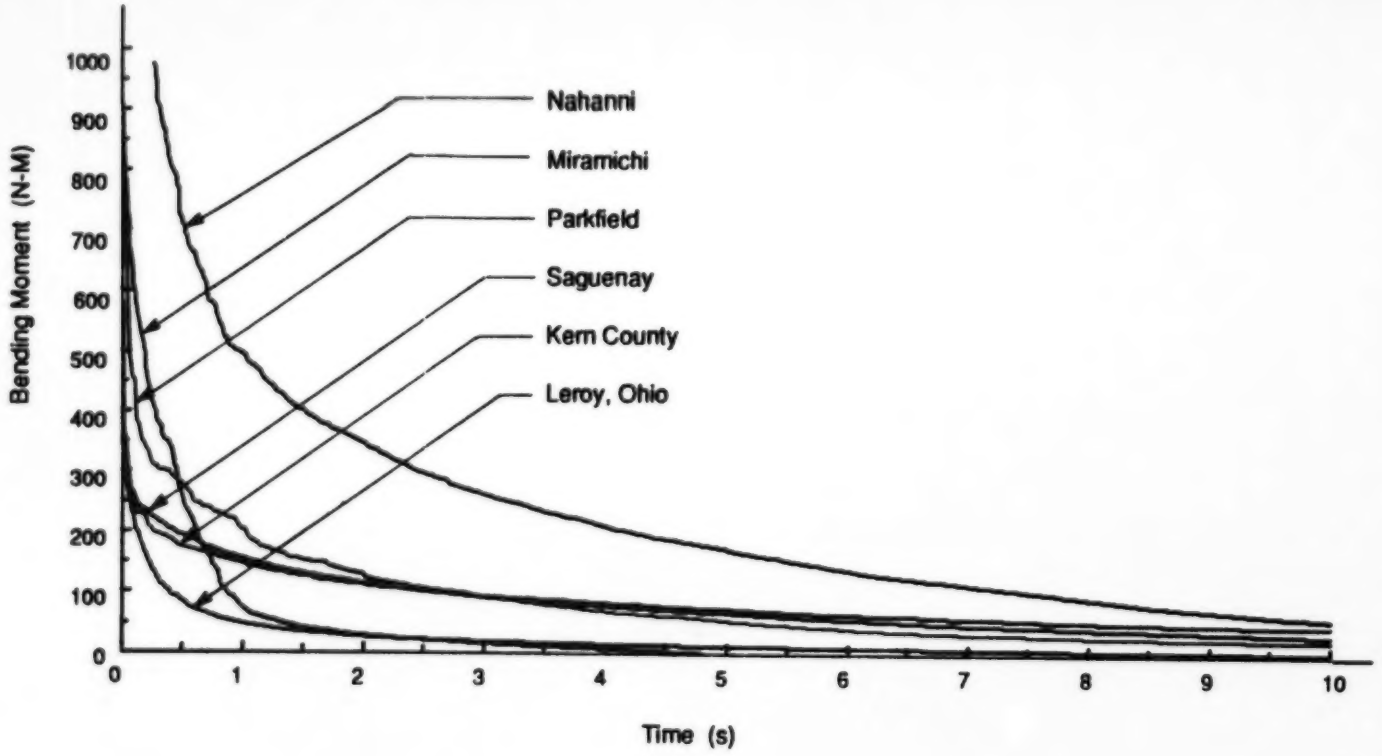


Fig. 16

Atomic Energy Control Board
The Effect of High Frequency Ground Motion on the Maple-X10 Reactor
Bending Moment Exceedance Curves at Node 2

ACRES

ENA accelerograms, the response spectra of such motion indicates that large forces would be induced.

However, since the duration of such motion is likely to be short, the time during which these forces are operative would be short. Most structures have sufficient energy absorption capability to withstand large, short-duration forces. This is confirmed mainly by observations and some analyses, as discussed in Ref 6. These higher forces may therefore not be damaging to the reactor. This should be confirmed by a detailed analysis of specific structures, in the Maple-X10 reactor.

# D. Conclusions and Recommendations

## 1. Conclusions

The following conclusions result from this study.

(1) Response spectra of ENA accelerograms indicate that significantly higher forces are induced in structures with high natural frequencies (>10 Hz) as compared to those induced by WNA accelerograms. However, the corresponding displacements are relatively small and the response spectra all fall below a blast damage threshold criterion.

(2) The selected high-frequency accelerograms results in a small amount of stored energy in low-natural frequency (<10 Hz) structures. This would explain the reason for the discrepancy between observed damage in low-natural frequency structures in ENA and damage predicted on the basis of peak motion.

(3) The energy induced in a structure with a high natural frequency subjected to high-frequency ground motion appears to be of comparable magnitude to that induced by low-frequency ground motion. Although this may imply similar damage potential, there are too few observed data to confirm this.

(4) Linear analyses of a high-natural frequency MDOF beam model also indicate that large forces would be induced by ENA accelerograms. However, comparison of the areas under the exceedance curves of bending moment in the beam suggests a relatively low damage potential for ENA accelerograms, depending on the threshold bending moment assumed for the structure.

(5) Measures of the damage potential of an accelerogram and of damage to a structural model depend greatly on the structure in question. Several criteria have been suggested, but those which account for the energy content of ground motion or the

energy dissipation and absorption in a structure, such as CAV, correlate best with observed damage.

(6) The Maple-X10 reactor core structure may have modes in the 15 - 30 Hz range. If subjected to high-frequency ground motion typical of ENA earthquakes, the induced forces at these frequencies would be larger than those induced by WNA ground motion. However, the resulting displacements would be relatively small (see Conclusion 1). Whether displacement or force affects survivability is still an area of active research.

(7) Application of a design response spectrum based on high-frequency ENA accelerograms to design or damage prediction in the high frequency range could be conservative since the response spectrum is a poor indicator of the energy available in ground motion. This is particularly true at high resonant frequencies since the duration of observed high-frequency ground motion is typically short and has small energy content. To avoid unnecessary conservatism, it may be necessary to modify either the response spectrum or the design procedure. This would apply to the Maple-X10 reactor core.

## 2. Recommendations

As a result of the literature review and study of linear SDOF and MDOF systems, it is recommended that a program of research into the effects of high-frequency ground motion on specific structures be undertaken. The basic purpose of the program is to derive modifications of design response spectra in the high-frequency (>10 Hz) range to avoid the possibility of overconservative design of structures with high natural frequencies. The following outlines the recommended research program.

(1) Obtain as many high-frequency ground motion accelerograms as possible. Generate artificial accelerograms consistent with an envelope of response spectra of the selected high-frequency ground motions.

(2) Nonlinear analyses of SDOF systems subjected to the selected accelerograms. This would provide a better understanding of the behavior of specific types of material models subjected to high-frequency ground motion and provide direction for the analysis of specific structures described below.

(3) Analyses of specific structures should be performed and, where possible, corroborated by observations. Reactor core structures and structures sensitive to large forces (e.g., porcelain insulators, weldments, relay switches) would be interesting candidate structures to analyze. The goal would be to establish appropriate design and damage prediction criteria for such structures.

(4) Develop modified response spectra for various ductility ratios which are representative of the response to ENA ground motion.

# REFERENCES

[1]Canadian Standards Association. Design Procedures for Seismic Qualification of CANDU Nuclear Power Plants. CSA Standard CAN3-N289.3-M81, 1981.

[2]Newmark, N.M. and Hall, W.J. Earthquake Spectra and Design. Earthquake Engineering Research Institute, Berkeley, Ca, 1982.

[3]Newmark, N.M., Blume, J.A. and Kapur, K.K. Seismic design spectra for nuclear power plants. J. Power Division, ASCE, 99, 287-303, 1973.

[4]Seed, H.B., Ugas, C. and Lysmer, J. Site-dependent spectra for earthquake-resistant design. Bull. Seis. Soc. Amer., 66, 221 - 243, 1976.

[5]Mohraz, B. A study of earthquake response spectra for different geological conditions. Bull. Seis. Soc. Amer., 66, 915 - 935, 1976.

[6]EPRI. A Criterion for Determining Exceedance of the Operating Basis Earthquake. Electric Power Research Institute, Palo Alto, Ca., Research Report NP-5930, 1988.

[7]Hanks, T.C., $f_{max}$. Bull. Seis. Soc. Amer., 72, 1867 - 1879, 1982.

[8]Somerville, P. Source scaling relations of large eastern North American earthquakes and implications for strong ground motions. In Proceedings from the Symposium on Seismic Hazards, Ground Motions, Soil Liquefaction and Engineering Practice in Eastern North America. National Center for Earthquake Engineering Research, SUNY, Buffalo, NY, 1987.

[9]Arias, A. A measure of earthquake intensity in seismic design of nuclear power plant. In Seismic Design of Nuclear Power Plants, MIT Press, 1970.

[10]Richter, C.A. Elementary Seismology. Freeman Publishing, 1958.

[11]Kennedy, R.P. Peak acceleration as a measure of damage. In Proceedings of the 4th International Seminar on Extreme Load Design of Nuclear Power Facilities, Paris, France, 1981.

[12]Kennedy, R.P. Engineering Characterization of Ground Motion, Task 1: Effects of Characteristics of Free-Field Motion on Structural Response. NUREG/CR-3805, 1984.

[13]Bolt, B.A. Duration of strong ground motions. In Proceedings of the 5th World Conference on Earthquake Engineering, Rome, 1973.

[14]Trifunac, M.D. and Brady, A.G., 1975. A study on the duration of strong earthquake ground motion. Bull. Seis. Soc. Amer., 65, 581 -626.

[15]Vanmarcke, E.H. and Lai, S.P. Strong Motion Duration of Earthquakes. Department of Civil Engineering, MIT, Publishing No. R77-16, 1977.

[16]Vanmarcke, E.H. and Lai, S.P. Strong motion duration and rms amplitude of earthquake records. Bull. Seis. Soc. Amer., 70, 1293 -1307, 1980.

[17]McCann, M.W. and Shah, H.C. Determining strong-motion duration of earthquakes. Bull. Seis. Soc. Amer., 69, 1253 - 1265, 1979.

[18]US Nuclear Regulatory Commission. Seismic and Geologic Siting Criteria for Nuclear Power Plants. 10 CFR Part 100, Appendix A, Federal Register, 38, No. 31282. 1973.

[19]Powell, G.H. and Allahabadi, R. Seismic damage prediction by deterministic methods: Concepts and Procedures. Earthquake Engineering and Structural Dynamics, 16, 719 - 734. 1988.

[20]Lew, T.K. and Takahashi, S.K. Rapid Seismic Analysis Procedure. Report No. 51-78-02, Naval Facilities Engineering Command. Port Hueneme, Ca, 1978.

[21]Hasselman, T.K., Eguchi, R.T. and Wiggins, J.H. Assessment of Damagability of Existing Buildings in a Natural Hazards Environment. Tech Report No. 80-1332-1. J.H. Wiggins Co., 1980.

[22]Kennedy, R.P., Short, S.A. and Newmark, N.M. The Response of a Nuclear Power Plant to Near-Field Moderate Magnitude Earthquakes. In transactions of the 6th International Conference on Structural Mechanics in Reactor Technology, V. K.(a), 1981.

[23]National Building Code of Canada, 1985.

[24]Veletsos, A.S. and Newmark, N.M. Effect of inelastic behavior on the response of simple systems to earthquake motions. In Proceedings of the Second World Conference on Earthquake Engineering, Tokyo, Japan, 1960.

[25]Veletsos, A.S., Newmark, N.M. and Chelapati, C.V. Deformation spectra for elastic and elastoplastic systems subjected to ground shock and earthquake motions. In Proceedings of the Third World Conference on Earthquake Engineering, New Zealand, 1965.

[26]Veletsos, A.S. Maximum deformations of certain nonlinear systems. In Proceedings of the Fourth World Conference on Earthquake Engineering, Santiago Chile, 1969.

[27]Newmark, N.M. and Hall, W.J. Vibrations of structures induced by ground motion. In Shock and Vibration Handbook (C.M. Harris and C.E. Crede, eds). McGraw Hill. 1976.

[28]Clough, R.W. and Penzien, J. Dynamics of Structures. McGraw-Hill, 1975.

[29]Kasiraj, I. and Yao, J.T.P. Expected fatigue damage of seismic structures. J. Structural Engineering, ASCE, 95, 1673 - 1692, 1972.

[30]Tang, J. P. and Yao, J.T.P. Expected fatigue damage of seismic structures. J. Engineering Mechanics, ASCE, 98, 695 - 709, 1972.

[31]Suidan, M.T. and Eubanks, R.A. Cumulative fatigue damage in seismic structures. J. Structural Engineering, ASCE, 99, 923 - 943, 1973.

[32]Zahrah, T.F. and Hall, W.J. Earthquake energy absorption in SDOF structures. J. Structural Engineering, ASCE, 110, 1757 - 1771, 1984.

[33]Zahrah, T.F. and Hall, W.J. Seismic energy absorption in simple structures. Report No. UILU-ENG-82-2011, Department of Civil Engineering, University of Illinois, 1982.

[34]Zhu, T.J., Tso, W.K. and Heidebrecht, A.C. Effect of peak ground a/v ratio on structural damage. J. Structural Engineering, ASCE, 114, 1019-1037, 1988.

[35]Dowding, C.H. Blast Vibration Monitoring and Control. Prentice-Hall, 1985.

[36]Edwards, A.T. and Northwood, T.D. Experimental studies of the effects of blasting on structures. The Engineer, 210, 538-546, 1960.

[37]Ang, A. H.S. and Wen, Y.K. Prediction of structural damage under random earthquake excitations. In Earthquake Ground Motion and Its Effects on Structures, ASME, AMD. Vol 53, 1982.

[38]Andreaus, U., Ceradini, G., D'Asdia, P., and Gaudenzi, P. Damage modeling and seismic response of simple degrading systems. Res. Mechanica, 22, 79-100, 1987.

[39]Park, Y.J. and Ang. A.H.S. Mechanistic seismic damage model for reinforced concrete. J. Structural Engineering, ASCE, 111, 722-739, 1985.

[40]Jeong, G.D. and Iwan, W.D. Effect of earthquake duration on the damage of structures. Earthquake Eng. Struct. Dyn., 16, 1201-1211, 1988.

[41]Bathe, K.J., Wilson, E.L. and Peterson, F.E. SAP IV, A Structural Analysis Program for Static and Dynamic Response of Linear Systems, Report NO. EERC 73-11, Earthquake Engineering Research Center, Berkeley, Ca, I1973.

[42]McGuire, R.K. and Barnhard, T.P. Four Definitions of Strong Motion Duration: Their Predictability and Utility for Seismic Hazard Analysis. US Geol. Survey, Open-File Report 79-1515, 1979.

# Appendix A

# Response Spectra

## APPENDIX A

### Response Spectra

The equation of motion of the damped single degree of freedom oscillator shown in Figure A-1 is

$$m\ddot{u}(t) + c\dot{u}(t) + ku(t) = -ma(t) \tag{1}$$

where $m$ is the mass of the oscillator, $c$ is its damping coefficient and $k$ is the stiffness of the spring. The forcing function is an accelerogram $a(t)$ which results in a relative displacement $u$ of the oscillator. Dividing Equation 1 by the mass $m$ and making the substitutions

$$\omega_0 = \sqrt{\frac{k}{m}} = 2\pi f_0$$
$$\beta = \frac{c}{2m\omega_0}$$

where $\omega_0$ is the natural angular frequency of the oscillator in radians/s and $\beta$ is the damping ratio expressed as a fraction of critical damping, results in the equation

$$\ddot{u}(t) + 2\beta\omega_0\dot{u}(t) + \omega_0^2 u(t) = -a(t) \tag{2}$$

Critical damping occurs when $\beta = 1$. In this case, when subjected to a displacement, the mass will simply return to its equilibrium position without oscillation.

The solution of Equation 2 is given by the Duhamel integral [Refs 2,7]

$$u(t) = -\frac{1}{\omega_0\sqrt{1-\beta^2}} \int_0^t a(\tau)e^{-\omega_0\beta(t-\tau)} \sin[\omega_0\sqrt{1-\beta^2}(t-\tau)]d\tau \tag{3}$$

where $u(0) = \dot{u}(0) = 0$. Differentiating Equation 3 with respect to $t$ results in the relative velocity response history, $\dot{u}(t)$ and the relative acceleration response history $\ddot{u}(t)$

$$\dot{u}(t) = -\int_0^t a(\tau)e^{-\omega_0\beta(t-\tau)} \cos[\omega_0\sqrt{1-\beta^2}(t-\tau)]d\tau + \frac{\beta}{\sqrt{1-\beta^2}} \int_0^t a(\tau)e^{-\omega_0\beta(t-\tau)} \sin[\omega_0\sqrt{1-\beta^2}(t-\tau)]d\tau$$

$$\ddot{u}(t) = \frac{\omega_0(1-2\beta^2)}{\sqrt{1-\beta^2}} \int_0^t a(\tau)e^{-\omega_0\beta(t-\tau)} \sin[\omega_0\sqrt{1-\beta^2}(t-\tau)]d\tau + 2\omega_0\beta \int_0^t a(\tau)e^{-\omega_0\beta(t-\tau)} \cos[\omega_0\sqrt{1-\beta^2}(t-\tau)]d\tau$$

The latter is not meaningful in terms of an effect on the oscillator. The absolute acceleration $\ddot{z}(t)$ is a measure of the force applied to the mass and is given by Equation 2

$$\ddot{z}(t) = \ddot{u}(t) + a(t) = -[2\beta\omega_0\dot{u}(t) + \omega_0^2 u(t)]$$

Many structures can be thought of as assemblages of single degree of freedom oscillators. The response of each oscillator can be characterized by the maximum absolute value of its relative displacement, velocity or acceleration time history. This leads to the concept of the response spectrum of an accelerogram which is the maximum absolute value of the response of a single

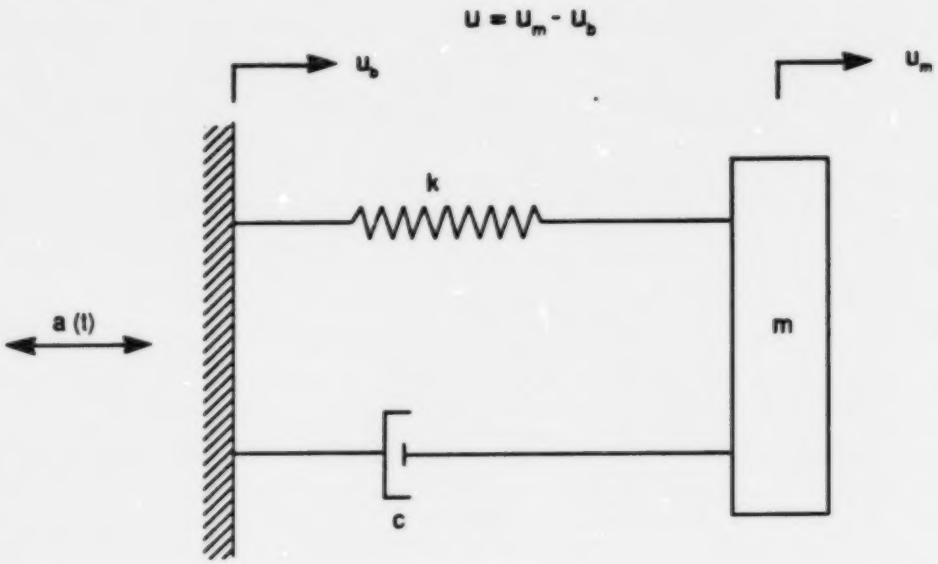


Fig. A-1

Atomic Energy Control Board
The Effect of High Frequency Ground Motion on the Maple-X10 Reactor
Damped Single Degree of Freedom Oscillator

ACRES

degree of freedom oscillator to the accelerogram as a function of oscillator frequency and damping. Displacement, velocity and acceleration response spectra may be defined

$$S_d(f_0,\beta) = \max_t |u(t,f_0,\beta)| \tag{4a}$$

$$S_v(f_0,\beta) = \max_t |\dot{u}(t,f_0,\beta)| \tag{4b}$$

$$S_a(f_0,\beta) = \max_t |\ddot{x}(t,f_0,\beta)| \tag{4c}$$

The procedure for computing $S_d$ is illustrated in Figure A-2. An algorithm for numerical computation of the response spectrum is given in Ref 7.

The maximum force in the spring of the oscillator is $kS_d = m\omega_0^2 S_d$. The quantity $\omega_0^2 S_d$ has units of acceleration and is known as the pseudo-acceleration, $PSA$. Pseudo-velocity is similarly defined. Thus

$$PSA = \omega_0^2 S_d$$
$$PSV = \omega_0 S_d$$

For low values of damping $PSA$ and $PSV$ are good approximations to $S_v$ and $S_a$. In fact, for $\beta = 0$, $PSA = S_a$. The approximation $PSV \approx S_v$ is good when the duration of the accelerogram is long compared to the oscillator period. Quantities related by powers of $\omega_0$ such as $S_d$, $PSV$ and $PSA$ can be plotted on four-way log paper as shown in Figures 4-1 and 4-2 of the main text, for example.

The use of the prefix 'pseudo' in connection with velocity and acceleration spectra is somewhat misleading since there is nothing false or incorrect about $PSV$ and $PSA$; they are merely approximations to $S_v$ and $S_a$.

*Energy Input and Absorption*

The energy input and absorption of the oscillator may be computed from the equation of motion 2. The energy input per unit mass, $E_i$, is given by multiplying the input acceleration $a(t)$ by the incremental displacement $du$ and integrating over the total displacement

$$E_i = -\int_0^u a\,du = -\int_0^t a(\tau)\dot{u}(\tau)d\tau$$

where $du = \dot{u}dt$. $E_i$ must be equal to the energy absorbed by various mechanisms. Integration of the left hand side of Equation 2 with respect to displacement yields

$$E_i = \int_0^u \ddot{u}du + 2\beta\omega_0 \int_0^u \dot{u}du + \omega_0^2 \int_0^u u\,du$$
$$= E_k + E_d + E_s$$

where $E_k$ is the kinetic energy of the mass, $E_d$ is the energy absorbed by the damper and $E_p$ is the potential (or strain) energy in the spring. The stored energy, $E_s$, is the sum of $E_k$ and $E_p$. Substituting $du = \dot{u}dt$ and integrating this sum by parts results in an expression for $E_s$ in terms of the displacement and velocity response

$$E_s(t) = \int_0^t \ddot{u}(\tau)\dot{u}(\tau)d\tau + \omega_0^2 \int_0^t u(\tau)\dot{u}(\tau)d\tau$$
$$= \frac{1}{2}\left[\dot{u}^2(t) + \omega_0^2 u^2(t)\right]$$

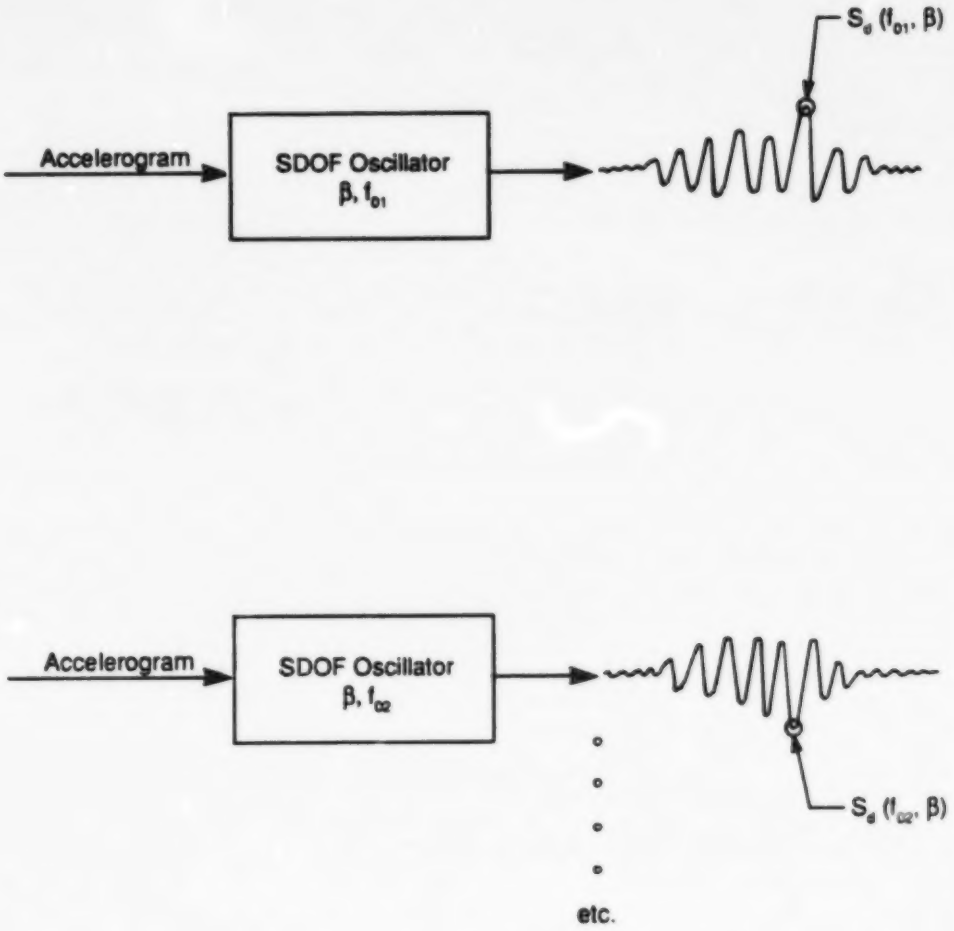


A plot of $S_d$ versus frequency is the displacement response spectrum.

Fig. A-2

Atomic Energy Control Board
The Effect of High Frequency Ground Motion on the Maple-X10 Reactor
Computation of Response Spectra

Response spectra of $E_s$ may be defined in a similar manner to response spectra of displacement, velocity and acceleration responses.

*Response Spectrum Limits and Bounds*

Response spectra of earthquake accelerograms tend to certain limits depending on the frequency of the oscillator and the frequency content of the ground motion. At all frequencies a certain amount of displacement of the spring is required to transmit enough force to overcome the inertia of the mass. At low oscillator frequencies relative to the dominant frequencies of the ground motion, the spring is flexible and more relative displacement must occur to transmit the required force. For most earthquake induced ground motion, the peak relative displacement of the mass tends toward the peak ground displacement as the oscillator frequency decreases to values less than 0.5 Hz. Conversely, at high oscillator frequencies relative to the dominant frequencies of the ground motion, the spring is stiff and only a small relative displacement will transmit the required force. For earthquake induced ground motion, the peak acceleration of the mass tends toward the peak ground acceleration as the oscillator frequency increases to values exceeding 20 Hz.

For earthquakes in western North America, the frequency at which the peak response of the oscillator is equal to the peak ground acceleration is about 33 Hz [Refs 5,6]. However, for earthquakes in eastern North America, the corresponding frequency bound seems to be higher.

These limits naturally divide the response spectra of earthquake accelerograms into displacement (low frequency), velocity (intermediate frequency) and acceleration (high frequency) portions. The peak response in each of these portions can be approximated as a multiple, depending on damping level, of the corresponding peak values of ground motion. This is the basis of the standard spectral shapes developed by Newmark and Hall as well as others [see Refs 4,5,6 and 8].

With regard to standard spectra, it should be noted that while the basic principles outlined in the preceding paragraphs apply to all response spectra, the actual values of the frequency limits as well as spectral shape have been found to depend on foundation soil type as well as earthquake magnitude and epicentral distance [Refs 4,8]. More recent efforts are aimed at predicting response spectral ordinates directly from attenuation relationships involving magnitude and epicentral distance [Refs 1,3].

**References**

[1] EPRI. *Modeling of Ground Motion Attenuation in Eastern North America*, Electric Power Research Institute, Palo Alto, Ca., Research Report NP-5577, 1988.

[2] Hudson, D. E. *Reading and Interpreting Strong Motion Accelerograms*, Earthquake Engineering Research Institute, Berkeley, Ca., 1979.

[3] Joyner, W. B. and Boore, D. M. Measurement, characterization and prediction of strong ground motion, in *Proceedings of Conference on Earthquake Engineering and Soil Dynamics, II*, (Park City, Utah), Technical Topics Division, ASCE, 1988.

[4] Mohraz, B. A study of earthquake response spectra for different geological conditions, *Bull. Seis. Soc. Amer.*, 66, 915-935, 1976.

[5] Newmark, N. M. and Hall, W. J. *Earthquake Spectra and Design*, Earthquake Engineering Research Institute, Berkeley, Ca., 1982.

[6] Newmark, N. M., Blume, J. A. and Kapur, K. K. Seismic design spectra for nuclear power plants, *J. Power Division, ASCE*, 99, 287-303, 1973.

[7] Nigam, N. C. and Jennings, P. C. Calculation of response spectra from strong motion earthquake records, *Bull. Seis. Soc. Amer.*, 59, 909-922, 1969.

[8] Seed, H. B., Ugas, C. and Lysmer, J. Site-dependent spectra for earthquake resistant design, *Bull. Seis. Soc. Amer.*, 66, 221-243, 1976.